

Optimization of N-Substituted Oseltamivir Derivatives as Potent Inhibitors of Group-1 and -2 Influenza A Neuraminidases, Including a Drug-Resistant Variant

Jian Zhang, Vasanthanathan Poongavanam, Dongwei Kang, Chiara Bertagnin, Huamei Lu, Xiujie Kong, Han Ju, Xueyi Lu, Ping Gao, Ye Tian, Haiyong Jia, Samuel Desta, Xiao Ding, Lin Sun, Zengjun Fang, Boshi Huang, Xuewu Liang, Ruifang Jia, Xiuli Ma, Wenfang Xu, Natarajan Arul Murugan, Arianna Loregian, Bing Huang, Peng Zhan, and Xinyong Liu

J. Med. Chem., **Just Accepted Manuscript** • DOI: 10.1021/acs.jmedchem.8b00929 • Publication Date (Web): 02 Jul 2018

Downloaded from <http://pubs.acs.org> on July 2, 2018

Just Accepted

“Just Accepted” manuscripts have been peer-reviewed and accepted for publication. They are posted online prior to technical editing, formatting for publication and author proofing. The American Chemical Society provides “Just Accepted” as a service to the research community to expedite the dissemination of scientific material as soon as possible after acceptance. “Just Accepted” manuscripts appear in full in PDF format accompanied by an HTML abstract. “Just Accepted” manuscripts have been fully peer reviewed, but should not be considered the official version of record. They are citable by the Digital Object Identifier (DOI®). “Just Accepted” is an optional service offered to authors. Therefore, the “Just Accepted” Web site may not include all articles that will be published in the journal. After a manuscript is technically edited and formatted, it will be removed from the “Just Accepted” Web site and published as an ASAP article. Note that technical editing may introduce minor changes to the manuscript text and/or graphics which could affect content, and all legal disclaimers and ethical guidelines that apply to the journal pertain. ACS cannot be held responsible for errors or consequences arising from the use of information contained in these “Just Accepted” manuscripts.

1
2
3
4
5
6
7
8
9
10
11
12
13
14
15
16
17
18
19
20
21
22
23
24
25
26
27
28
29
30
31
32
33
34
35
36
37
38
39
40
41
42
43
44
45
46
47
48
49
50
51
52
53
54
55
56
57
58
59
60

	Sciences, Shandong University Ma, Xiuli; Institute of Poultry Science, Shandong Academy of Agricultural Sciences Xu, Wenfang; Shandong Univ, School of Pharmaceutical Sciences, Shandong University, Department of Medicinal Chemistry Murugan, Natarajan Arul; Division of Theoretical Chemistry and Biology, School of Biotechnology, KTH Royal Institute of Technology Loregian, Arianna; University of Padova, huang, bing; Shandong Academy of Agricultural Sciences, Institute of Poultry Science Zhan, Peng; Shandong Univ, Liu, Xinyong; School of Pharmaceutical Sciences, Shandong University, Department of Medicinal Chemistry
--	---

SCHOLARONE™
Manuscripts

1
2
3
4
5
6
7
8
9
10
11
12
13
14
15
16
17
18
19
20
21
22

Optimization of N-Substituted Oseltamivir Derivatives as Potent Inhibitors of Group-1 and -2 Influenza A Neuraminidases, Including a Drug-Resistant Variant

23
24
25
26
27
28
29
30
31
32
33
34
35
36
37
38
39
40
41
42
43
44
45
46
47
48
49
50
51
52
53
54
55
56
57
58
59
60

Jian Zhang,[†] Vasanthanathan Poongavanam,[‡] Dongwei Kang,[†] Chiara Bertagnin,[&]
Huamei Lu,[‡] Xiujie Kong,[†] Han Ju,[†] Xueyi Lu,[†] Ping Gao,[†] Ye Tian,[†] Haiyong Jia,[†]
Samuel Desta,[†] Xiao Ding,[†] Lin Sun,[†] Zengjun Fang,^{†,‡,#} Boshi Huang,[†] Xuewu Liang,[†]
Ruifang Jia,[†] Xiuli Ma,[‡] Wenfang Xu,[†] Natarajan Arul Murugan,[≠] Arianna Loregian,[&]
Bing Huang,^{‡,*} Peng Zhan,^{†,*} and Xinyong Liu^{†,*}

[†] *Department of Medicinal Chemistry, Key Laboratory of Chemical Biology (Ministry of Education), School of Pharmaceutical Sciences, Shandong University, 44 West Culture Road, 250012 Jinan, Shandong, PR China.*

[‡] *Institute of Poultry Science, Shandong Academy of Agricultural Sciences, 1, Jiaoxiao Road, Jinan, Shandong 250023, P. R. China.*

[&] *Department of Molecular Medicine, University of Padova, via Gabelli 63, 35121 Padova, Italy*

[‡] *Department of Physics, Chemistry, and Pharmacy, University of Southern Denmark, DK-5230 Odense M. Denmark.*

[≠] *Division of Theoretical Chemistry and Biology, School of Biotechnology, KTH Royal Institute of Technology, S-106 91 Stockholm, Sweden.*

[#] *The Second Hospital of Shandong University, No. 247 Beiyuan Avenue, Jinan 250033, China.*

1
2
3
4 **ABSTRACT:** Based on our earlier discovery of N1-selective inhibitors, the
5
6 150-cavity of influenza virus neuraminidases (NAs) could be further exploited to
7
8 yield more potent oseltamivir derivatives. Among the synthesized compounds, **15b**
9
10 and **15c** were exceptionally active against both group-1 and -2 NAs. Especially for
11
12 09N1, N2, N6 and N9 subtypes, they showed 6.80-12.47 and 1.20-3.94 times greater
13
14 activity than oseltamivir carboxylate (OSC). They also showed greater inhibitory
15
16 activity than OSC towards H274Y and E119V variant. In cellular assays, they
17
18 exhibited greater potency than OSC towards H5N1, H5N2, H5N6, and H5N8 viruses.
19
20
21 **15b** demonstrated high metabolic stability, low cytotoxicity *in vitro*, and low acute
22
23 toxicity in mice. Computational modeling and molecular dynamics studies provided
24
25 insights into the role of R group of **15b** in improving potency towards group-1 and -2
26
27 NAs. We believe the successful exploitation of the 150-cavity of NAs represents an
28
29 important breakthrough in the development of more potent anti-influenza agents.
30
31
32
33
34
35
36
37
38
39
40
41
42
43
44
45
46
47
48
49
50
51
52
53
54
55
56
57
58
59
60

INTRODUCTION

Influenza A virus is the pathogenic agent of seasonal, occasional, and pandemic influenza in both humans and animals, causing acute contagious respiratory infections that may be life-threatening or even lethal.¹⁻³ According to the World Health Organization (WHO, 2018), the annual incidence of severe illness is about 3 to 5 million cases, with about 290,000 to 650,000 deaths.⁴ Currently, two subtypes influenza A virus (H1N1pdm09 and H3N2) are the predominant circulating strains responsible for annual/seasonal influenza epidemics.⁴ The influenza A virus has been the causative agent of five major pandemics in the last century and the beginning of this century: the 1918 Spanish flu (H1N1), 1957 Asian flu (H2N2), 1968 Hong Kong flu (H3N2), 1977 Russian flu (H1N1), and 2009 swine-origin pandemic flu (H1N1pdm09).⁵⁻⁷

Avian influenza virus (AIV), which belongs to the influenza A virus family, has caused substantial economic losses throughout the world due to high bird mortality and the cost of control measures to prevent its spread in poultry.⁸ In general, AIV strains have strong host-species barriers,¹¹ but nevertheless, human and mammals are often infected with various AIV subtypes, including H5N1, H5N2, H5N6, H6N1, H7N9, and H9N2 strains.¹²⁻¹⁵ In particular, H5N1 and H7N9 (first identified in China in March 2013) showed mortality rates of 60% and 40%, respectively, in humans. Though their mode of transmission is not yet fully established, and there is no clear evidence of efficient human-to-human transmission,^{14,16} the worrying possibility remains that further adaptation of AIV for person-to-person transmission could give

1
2
3
4 rise to a worldwide pandemic.

5
6 Influenza A viruses contain two important surface antigenic glycoproteins,
7
8 hemagglutinin (HA) and neuraminidase (NA).¹⁷ Different subtypes are named
9
10 according to the antigenic properties of the HA and NA molecules. In terms of NA,
11
12 influenza A viruses can be classified into N1-N11 subtypes.¹⁸ NAs play an essential
13
14 role in the release of newly formed virions from infected cells and facilitate
15
16 propagation of the virus,^{19,20} therefore, NAs are promising targets for anti-influenza
17
18 drugs.²¹ Indeed, several neuraminidases inhibitors (NAIs) have been approved for
19
20 clinical use, including oseltamivir (**1** Tamiflu[®]),²² zanamivir (**2** Relenza[®]),²³
21
22 laninamivir octanoate (**3** Inavir[®])²⁴ and peramivir (**4** Rapivab[®])²⁵ (Figure 1). Among
23
24 the approved drugs, only oseltamivir (a prodrug of oseltamivir carboxylate) (OSC) is
25
26 orally available, and it has been a first-line therapy since its approval in 1999. Other
27
28 neuraminidase inhibitors are mainly administered by inhalation or intravenously due
29
30 to their high polarity.²⁵ However, various mutants with resistance to these four drugs
31
32 have appeared,²⁶⁻²⁹ such as the most frequent NA substitutions reported in H5N1
33
34 (H274Y) and H3N2 (E119V) subtypes confer resistance to oseltamivir without
35
36 altering susceptibility to zanamivir, which have severely limited Tamiflu's clinical
37
38 application.^{26,28,29} For NA of H5N1-H274Y mutant, Collins *et al.*²⁷ revealed the
39
40 molecular basis of the oseltamivir resistance of His274Y, suggesting that the mutation
41
42 of histidine to a bulkier tyrosine residue could disorder the hydrophobic pocket
43
44 formed by the methylene of Glu276, thus preventing OSC from making hydrophobic
45
46 contact with the ligand-binding pocket. Thus, there is an urgent need to develop
47
48
49
50
51
52
53
54
55
56
57
58
59
60

improved NAIs for effective influenza therapy.

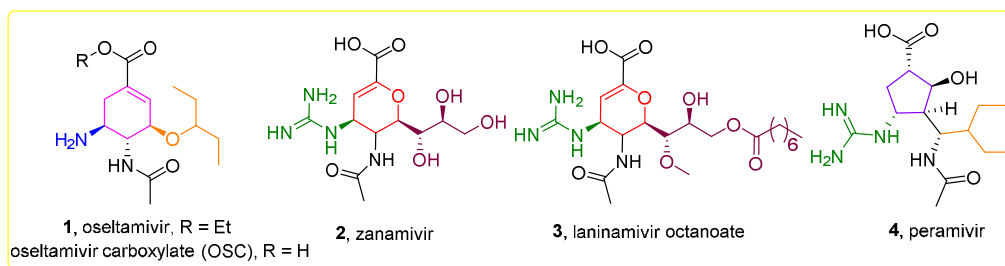


Figure 1. Structures of the licensed NA inhibitors 1-4

Typically, the classic NA inhibitors were designed based on the crystal structures of NAs. Based on the phylogenetic tree, the N1-N9 subtypes can be divided into two groups: group-1 (N1, N4, N5, and N8), and group-2 (N2, N3, N6, N7, and N9) (see Supporting Information, Figure S1).³⁰ For group-1 NAs (except pH1N1 (09N1)), the crystal structures reveal that the 150-loop, containing residues 147-152, adopts an open conformation, forming the 150-cavity adjacent to the active site. In contrast, no group-2 NA has yet been crystallographically shown to have the 150-loop in a completely open conformation. As exemplified by N2, there is a key salt bridge between the conserved residues Asp147 and His150, which was considered to lock the 150-loop in the closed conformation and to control the formation of the 150-cavity.^{31,32} However, in contrast to the other characterized N1 subtypes, 09N1 does not have an open 150-cavity,³³ and this surprising finding suggested that the 09N1 150-loop closely resembles that of group-2 rather than group-1 NAs. Therefore, except for 09N1, the 150-cavity is a unique feature of group-1 NAs. Various compounds, such as C-5 amino-substituted oseltamivir derivatives **5**, **6**,³⁴ and **7**,³⁵ (N1-selective, more potent than OSC), oseltamivir analogues **8**,³⁶ (N1-selective, less potent than zanamivir), sialic acid derivative **9**,³⁷ (N1-selective, less potent than

zanamivir and sialic acid), zanamivir derivative **10**,³⁸ (less potent than zanamivir) and C-6 substituted oseltamivir derivatives **11** and **12**³⁹ (H3N2-selective) have been discovered to target the 150-cavity of NAs (Figure 2).

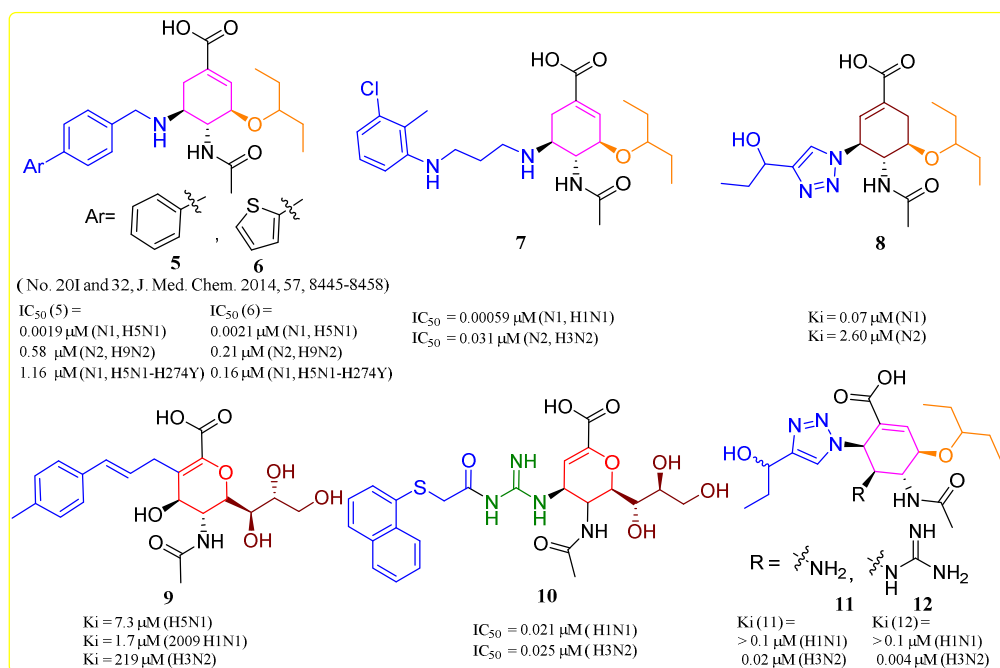


Figure 2. Structures of the group-1-specific influenza NA inhibitors **5-10** and H3N2-selective inhibitors **11** and **12**.

Recently, molecular dynamics (MD) simulation studies indicated that the conformation of the 150-loop in group-1 NAs could generate an even more extended 150-cavity than that observed in the crystal structures.^{31,40,41} Similarly, the flexibility of the 150-loop of 09N1 is very high, and biophysical simulations showed that the 09N1 favors an open 150-cavity conformation overall.⁴² In addition, the amino acid sequences of the group-1 and group-2 NA 150-loops show a high degree of similarity.³⁰ The recent crystal structure of a half-open 150-loop in a complex of N2 with OSC,³² and several computational studies further suggested that the conformation

1
2
3
4 of the 150-loop in NAs of both groups could be easily influenced by an introduced
5
6 ligand, which might interact with the closed 150-loop and lock it in an open
7
8 conformation.^{39, 42} Thus, the open 150-cavity may exist not only in group-1 NAs, but
9
10 also in group-2 NAs in the physiological situation. In other words, intrinsic protein
11
12 flexibility and ligand-induced protein flexibility could provide a basis for further
13
14 anti-influenza drug discovery *via* a structure-based approach.
15
16
17
18
19

20 **DESIGN OF OSELTAMIVIR DERIVATIVES**

21
22
23 The main objective of this research was to discover potent group-1 and group-2
24
25 NAIs as candidate anti-influenza agents by exploiting the 150-cavity adjacent to the
26
27 active site of influenza A viral NAs. As shown in Figure 3, the C-5 amino group and
28
29 C-6 of OSC in the NAs active site lie very close to the open 150-cavity of group-1
30
31 NAs (1918H1N1, H5N1, and H5N8) and the closed 150-loop of 09N1 and group-2
32
33 NAs (H3N2, H5N2, H5N6, and H7N9). The C-6 substituted oseltamivir derivatives
34
35 **11** and **12** were designed to target both the active site and the 150-cavity of group-1
36
37 and -2 NAs, but the results were unsatisfactory, even though they showed potent
38
39 H3N2-selective inhibitory activity.³⁹ On the other hand, C-5 amino-substituted
40
41 oseltamivir derivatives (**5**, **6**, and **7**) were potent N1-selective inhibitors, being more
42
43 potent than OSC against N1.³⁴⁻³⁶ Moreover, at high concentration, the deprotonated
44
45 C-5 amino group of OSC exerts a significant effect on the rigid closed N2 150-loop
46
47 and can induce half-opening.³² So, we set out to modify the C-5 amino group of
48
49 oseltamivir, aiming to probe the group-1 NAs 150-cavity and to force the unexplored
50
51
52
53
54
55
56
57
58
59
60

closed 150-cavity of 09N1 and group-2 NAs into open conformation.

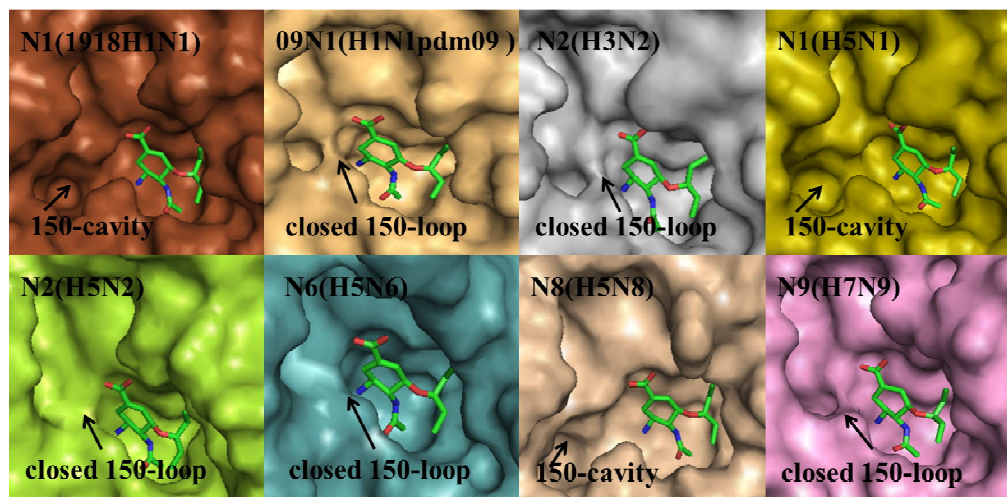


Figure 3. Comparison of the crystal structures of the NA subtypes used in our NA inhibition assay, bound with OSC. Structures of N1 (1918H1N1, PDB ID: 3BEQ), 09N1 (H1N1pdm09, PDB ID: 3TI6), N2 (H3N2, PDB ID: 4GZP), N1 (H5N1, PDB ID: 2HU0), N2 (H5N2, PDB ID: 5HUK), N6 (H5N6 PDB ID: 5HUM), N8 (H5N8, PDB ID: 2HT7) and N9 (H7N9, PDB ID: 5L15) are in surface representation. It can be seen that 09N1 (H1N1pdm09), along with N2, N6, and N9 have a closed 150-loop, but N1 and N8 have an open 150-cavity.

Our previous report revealed that structure-based design of specific N1 inhibitors targeting the activity site and 150-cavity was a successful strategy for discovering anti-influenza agents, such as **5** and **6** (lead compounds, originally numbered 20I and 32, *J. Med. Chem.* 2014, 57, 8445-8458), which contain hydrophobic *p*-phenyl and *p*-(thiophen-2-yl)-benzyl groups, respectively, and exhibit more potent N1-selective inhibition than OSC.³⁴ It turned out that the substituted benzyl group is an excellent privileged moiety for the 150-cavity.³⁴ Recent computational models of N1 have revealed that *N*-containing polar groups (including hydrazine, imineamide and amino derivatives) and bulky moieties (including aromatic rings, heterocyclic group and

1
2
3
4 alkene moieties) are available for hydrogen bond formation with Gly147, Val149, and
5
6 Asp151 and for van der Waals (vdW) interactions with Gln136, Asp151, and Thr439
7
8 in the 150-cavity, respectively. Consequently, an aromatic ring with polar moieties
9
10 may be sterically and electronically complementary to the 150-cavity.⁴³ In addition,
11
12 MD studies indicated that the triazole-containing oseltamivir analogs (**11** and **12**,³⁹
13
14 which were designed to adapt to the 150-cavity of N1 and N2, and showed higher
15
16 efficacy against H3N2 strain than H1N1 strain) could alternatively occupy the
17
18 150-cavity and the catalytic site of N1 or N2, because of the short triazole group and
19
20 the rigid and large angle between the central ring and the triazole group. Even so, it
21
22 was clear that the 150-cavity of group-2 could be induced to open by oseltamivir
23
24 derivatives, and *N*-containing groups (triazole group) play an important role in this
25
26 process.
27
28
29
30
31

32
33 Our strategy here was to explore and optimize the substituted benzyl structure of
34
35 lead compound **5** or **6** and to identify structure-activity relationships (SARs) that
36
37 could be utilized to improve the potency against both group-1 and -2 NAs while also
38
39 showing good potency against H5N1-274Y mutant, by introducing phenyl and
40
41 alkyl-substituted *N*-containing groups or *N*-containing aryl groups at the *para*-position
42
43 of the benzyl group of **5** or **6**. Thus, we designed and synthesized a series of C-5
44
45 amino-substituted oseltamivir derivatives (Figure 4), anticipating that 1) phenyl and
46
47 alkyl-substituted *N*-containing groups or *N*-containing aryl groups at the *para*-position
48
49 of the benzyl group would have sufficiently large size, sufficient length, relative
50
51 flexibility, and appropriate hydrophobicity to bind effectively to the 150-cavity of
52
53
54
55
56
57
58
59
60

group-1 NAs, 2) the 150-cavity of 09N1 and group-2 NAs is likely to be opened and bound by C-5 amino and substituted benzyl groups, and 3) the substituted benzyl group may form strong interactions with the 150-cavity of NAs of both groups to increase the affinity between the compounds and the targets and thus improve the anti-resistance profile. Given the importance of interactions between the substituted benzyl groups and 150-cavity, we were optimistic that these design and optimization strategies would be fruitful.

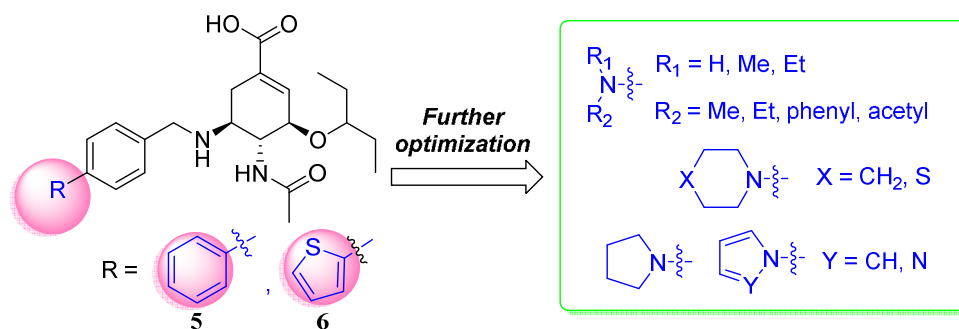


Figure 4. Further structural optimization of oseltamivir derivatives **5** and **6**.

CHEMISTRY

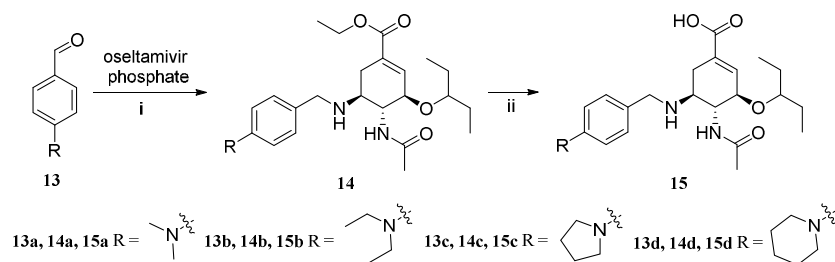
The synthetic protocols for the new oseltamivir derivatives are outlined in Schemes 1-6. All derivatives were synthesized by well-established methods using commercially available oseltamivir phosphate as the primary starting material. In Scheme 1, oseltamivir phosphate was treated with a series of different aldehydes in the presence of NaBH_3CN to afford the key intermediates **14a-14d**. Subsequently, **14a-14d** were hydrolyzed in the presence of NaOH aqueous solution and acidified with hydrochloric acid aqueous solution to give the corresponding target compounds **15a-15d**.

Compound **19** was synthesized according to the synthetic protocols in Scheme 2. 4-Thiomorpholinobenzaldehyde (**17**) was prepared by reaction of thiomorpholine with 4-fluorobenzaldehyde (**16**) in the presence of potassium carbonate. The target compound **19** was prepared *via* similar procedures from **15a-15d**. Compound **22** was obtained according to the method shown in Scheme 3.

A Buchwald-Hartwig cross-coupling reaction of the 4-bromobenzaldehyde with aniline, *N*-methyl or ethyl substituted aniline afforded another three aryl aldehydes **24a-24c**, which were transformed to the corresponding target compounds **26a-26c** (Scheme 4).

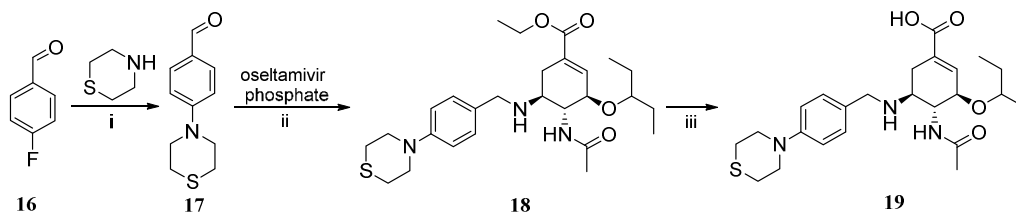
Compounds **29a-29b** were also prepared *via* similar procedures from **15a-15d**, as depicted in Scheme 5. Lead compound **6** (originally numbered **32**, *J. Med. Chem.* **2014**, *57*, 8445-8458) was obtained according to the method we previously reported.³⁴ All novel derivatives were fully characterized by electrospray ionization mass spectrometry (ESI-MS), high-resolution mass spectroscopy (HRMS), proton nuclear magnetic resonance (¹H NMR) spectroscopy, and carbon nuclear magnetic resonance (¹³C NMR) spectroscopy. The purity of all target compounds was >95% as determined by analytical HPLC.

Scheme 1. Synthesis of Compounds 15a-15d^a

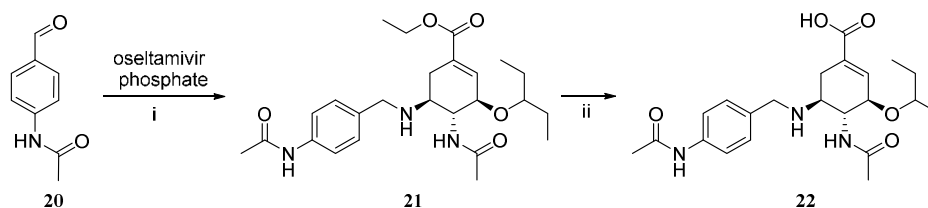


^a (i) NaBH₃CN, EtOH, MeOH, rt, 60-70%; (ii) NaOH, MeOH, H₂O, rt, then HCl (2 mol/L),

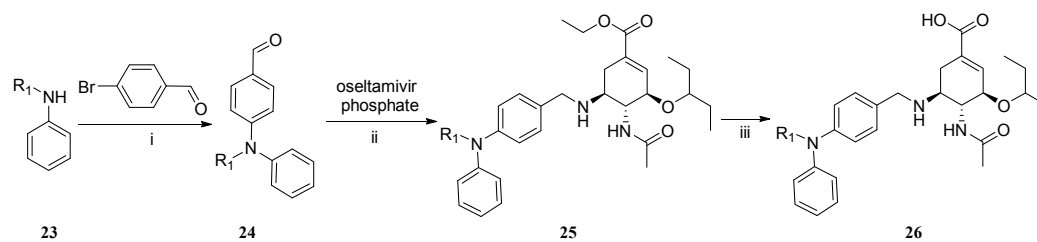
60-75%.

Scheme 2. Synthesis of Compound 19^a

^a (i) DMSO, K₂CO₃, 100-120°C, 4h, 68%; (ii) NaBH₃CN, EtOH, MeOH, rt, 63%; (iii) NaOH, MeOH, H₂O, rt, then HCl (2 mol/L), 60%.

Scheme 3. Synthesis of Compound 22^a

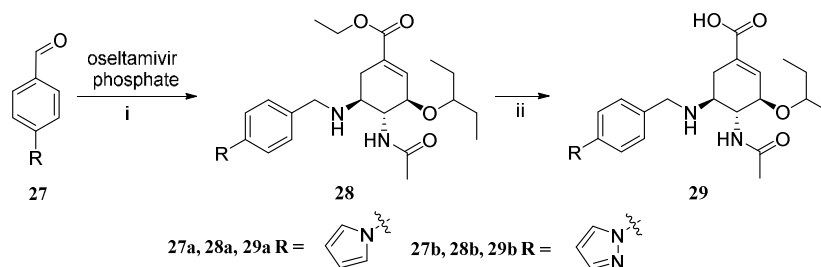
^a (i) NaBH₃CN, EtOH, MeOH, rt, 76%; (ii) NaOH, MeOH, H₂O, rt, then HCl (2 mol/L), 74%.

Scheme 4. Synthesis of Compounds 26a-26c^a

23a, 24a, 25a 26a R₁ = H; 23b, 24b, 25b, 26b R₁ = Me; 23c, 24c, 25c, 26c R₁ = Et.

^a (i) toluene, Cs₂CO₃, Pd(OAc)₂, BINAP, reflux, 60-70%; (ii) NaBH₃CN, EtOH, MeOH, rt, 60-70%; (iii) NaOH, MeOH, H₂O, rt, then HCl (2 mol/L), 58-70%.

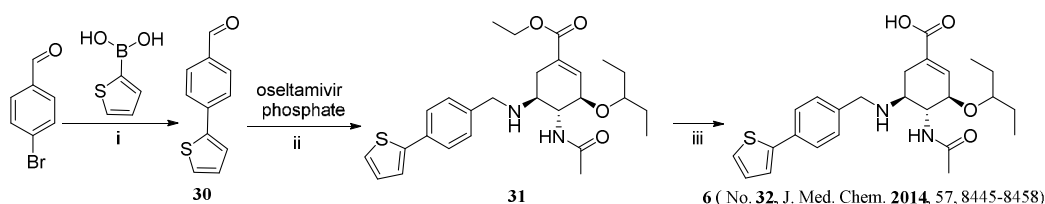
Scheme 5. Synthesis of Compounds 29a-29b^a



^a (i) NaBH₃CN, EtOH, MeOH, rt, 55-65%; (ii) NaOH, MeOH, H₂O, rt, then HCl (2 mol/L), 60-70%.

Scheme 6. Synthesis of Lead Compound 6 (originally numbered 32, J. Med.

Chem. 2014, 57, 8445-8458)^a



^a (i) DMSO, K₂CO₃, Pd(PPh₃)₄, reflux, 68%; (ii) NaBH₃CN, EtOH, MeOH, rt, 68%; (iii) NaOH, MeOH, H₂O, rt, then HCl (2 mol/L), 74%.

RESULTS AND DISCUSSION

Inhibition of Influenza Neuraminidases

All the newly designed oseltamivir derivatives were screened for NA-inhibitory activity using a chemiluminescence-based assay with 2'-(4-methylumbelliferyl)- α -D-N-acetylneuraminic acid (MUNANA) as the substrate.³⁴ For NA inhibition screening, we chose five NAs in each group (10 influenza subtypes in total): the endemic human strains seasonal H1N1, pandemic H1N1 (H1N1pdm09), and H3N2, which caused significant morbidity and mortality in

1
2
3 humans, and avian influenza viruses (H5N1, H5N2, H5N6, H5N8, H7N9, H9N2, and
4 oseltamivir-resistant H5N1-H274Y) that pose a significant threat to birds, poultry,
5 mammals and humans.^{5-7, 12-16} In addition to the reference compounds oseltamivir
6 carboxylate (OSC) and zanamivir, we also employed compound **6** as a reference,
7 since it has been reported to show selectivity for N1 over N2.³⁴ **Table 1** summarizes
8 the measured inhibition potencies of the synthesized compounds towards the above
9 NAs. It is clear that OSC showed greater inhibitory potency towards wild-type
10 group-1 NAs (IC_{50} = 4.45-33.56 nM) and group-2 NAs (IC_{50} = 4.17-15.72 nM).
11 However, OSC showed weaker activity towards the H5N1-H274Y mutant (IC_{50} =
12 1630 nM), as previously reported.^{34,44}

13
14
15
16
17
18
19
20
21
22
23
24
25
26
27
28 Impressively, several of the designed compounds had greater inhibitory potency
29 than the reference compounds, and in particular, **15b** showed single-digit nanomolar
30 activity against NAs of the H1N1, H1N1pdm09, H3N2, H5N2, H5N8, H9N2 and
31 H7N9 strains. However, compound **15a** exhibited weaker activity against NAs of
32 H5N1 (IC_{50} = 120.93 nM) and H5N6 (IC_{50} = 33.85 nM), showing approximately 3-
33 and 2-fold lower potency than OSC, respectively.

34
35
36
37
38
39
40
41
42
43 The inhibitory effects of **15b** and **15c** bearing *N,N*-diethylamino and
44 1-pyrrolidine groups, respectively, toward the nine wild NA subtypes lay within a
45 narrow concentration range (IC_{50} values ranging from 0.35 nM to 33.72 nM and 1.81
46 nM to 14.31 nM, respectively). In the case of H5N1 NA, the IC_{50} value of **15b** was
47 33.72 nM, which is similar to that of OSC (IC_{50} = 33.56 nM). As for the other eight
48 wild NA subtypes, **15b** turned out to be a highly potent inhibitor of both group-1 NAs
49
50
51
52
53
54
55
56
57
58
59
60

(H1N1, IC_{50} = 1.16 nM; H1N1pdm09, IC_{50} = 0.55 nM; H5N8, IC_{50} = 5.34 nM) and group-2 NAs (H3N2, IC_{50} = 1.05 nM; H5N2, IC_{50} = 0.49 nM; H9N2, IC_{50} = 0.35 nM; H5N6, IC_{50} = 1.26 nM; H7N9, IC_{50} = 1.79 nM), with greater potency than OSC or zanamivir. In addition, compound **15c** exhibited better inhibition of all wild-type NAs of group-1 (H1N1, IC_{50} = 2.65 nM; H1N1pdm09, IC_{50} = 2.31 nM; H5N1, IC_{50} = 14.31 nM; H5N8, IC_{50} = 4.06 nM) and group-2 (H3N2, IC_{50} = 1.81 nM; H5N2, IC_{50} = 4.50 nM; H9N2, IC_{50} = 2.13 nM; H5N6, IC_{50} = 10.85 nM; H7N9, IC_{50} = 6.51 nM), being 1.2 to 3.94-fold more potent than OSC. It is worth noting that the IC_{50} values of **15b** were much lower against the five NAs of group-2 (especially H7N9 NA) and 09N1 than against the three NAs of group-1. Indeed, the IC_{50} values of **15b** against NAs of H1N1pdm09, H3N2, H5N2, H5N6, H9N2 and H7N9 were approximately 8, 7, 11, 13, 13, and 6 times, and 8, 6, 27, 18, 26, and 10 times lower than those of OSC and zanamivir for the same NAs, respectively. In general, **15b** showed comparable or much better inhibitory activities relative to **15c** against both group-1 and -2 wild-type NAs, suggesting that the flexible *N,N*-diethylamino group at the R-position was more advantageous for NAs inhibitory activity than the rigid 1-pyrrolidine group.

The presence of the 1-piperidine group (**15d**) and 4-thiomorpholine group (**19**) resulted in decreased activities towards group-1 and -2 NAs (**15d**, IC_{50} = 16.64-165.90 nM; **19**, IC_{50} = 48.38-557.77 nM) in comparison with OSC. Moreover, neither compound displayed selectivity for group-1 or -2 NAs. Compared with **15d**, compound **19** was less potent against both group-1 and -2 wild-type NAs, demonstrating that replacing the 1-piperidine group with a 4-thiomorpholine group

1
2
3 resulted in reduced NA-inhibitory activity. Compound **22** ($IC_{50} = 10.91\text{-}581.03$ nM)
4
5 with an *N*-acetamide group at the R-position showed significantly reduced activity
6
7 against both group-1 and -2 wild-type strains, especially H5N1 ($IC_{50} = 581.03$ nM),
8
9 H5N2 ($IC_{50} = 31.73$ nM), H5N6 ($IC_{50} = 181.17$ nM), H5N8 ($IC_{50} = 216.53$ nM) and
10
11 H7N9 ($IC_{50} = 31.47$ nM) relative to **15a-15c**, OSC and zanamivir. Therefore, we did
12
13 not further explore amide groups as the R group of oseltamivir derivatives.
14
15
16
17

18 Based on the above information and our previously established structure-activity
19
20 relationships (SAR) results,^{34,43} we concluded that *N,N*-dialkyl-substituted aniline
21
22 derivatives preferentially bind to the 150-cavity of both group-1 and -2 NAs, and the
23
24 key factors influencing the activities are the size, flexibility and hydrophobicity of the
25
26 *N,N*-dialkyl substituted group. Compounds with *N,N*-diethylamino (**15b**) and
27
28 1-pyrrolidinyl groups (**15c**), which possess moderate size, flexibility, and
29
30 hydrophobicity, at the R-position enhanced the activities against both group-1 and -2
31
32 wild-type NAs, while relatively bulky, rigid (**15d** and **19**) or small (**15a**) substituent
33
34 groups appeared to have a negative effect on the potency, possibly because their
35
36 conformational effects impaired the binding of other structural parts of oseltamivir
37
38 derivatives to the corresponding pockets of the active site. In addition, an amide
39
40 substituent group reduced the activity, as exemplified by compound **22**.
41
42
43
44
45
46

47 To further examine the effects of N-substituted fragments, one of the two methyl
48
49 groups of **15a** or ethyl groups of **15b** was replaced with a phenyl group or a hydrogen
50
51 atom (cf. compounds **26a-26c**). Among them, compound **26b** (*N*-methylaniline
52
53 derivative) exhibited the most potent activity against NAs of H3N2 and H9N2 ($IC_{50} =$
54
55
56
57
58
59
60

1
2
3 5.65 nM and 2.29 nM, respectively), being more potent than the reference compounds.
4
5
6 It also exhibited similar potency towards NAs of H1N1 ($IC_{50} = 9.62$ nM),
7
8 H1N1pdm09 ($IC_{50} = 29.82$ nM), H5N2 ($IC_{50} = 62.84$ nM), H5N8 ($IC_{50} = 29.00$ nM),
9
10 and H7N9 ($IC_{50} = 11.37$ nM) relative to OSC and zanamivir, but was less potent than
11
12 OSC and zanamivir against NAs of H5N1 and H5N6. Nevertheless, **26a** ($IC_{50} =$
13
14 27.39 - 599.17 nM) and **26c** ($IC_{50} = 275.3$ - 2586 nM) showed significantly reduced
15
16 NA-inhibitory activity towards both group-1 and -2 wild-type NAs. These results
17
18 suggest that either too large (phenyl or ethyl), or too small (hydrogen atom) or too
19
20 rigid (phenyl) *N*-substituted groups are unfavorable for NA-inhibitory activity, in
21
22 accordance with the above-established SARs (i.e., relatively bulky, rigid or small
23
24 substituent groups appeared to have a negative effect on the potency).
25
26
27
28
29

30 In addition, we replaced the *N,N*-diethylamino group of **15b** with 1H-pyrrole and
31
32 1H-pyrazole groups (cf. **29a** and **29b**). Like reference compound **6**, **29a** and **29b**
33
34 turned out to be selective inhibitors of group-1 NAs (cf. Table 1). As per our
35
36 established SARs for this class of compound,³⁴ **29a** and **29b** showed significantly
37
38 decreased inhibitory activity for group-2 NAs (H3N2, H5N2, H5N6, H9N2, and
39
40 H7N9). It is noteworthy that **29a** was a much more potent inhibitor of both group-1
41
42 and 2 wild-type NAs (1.17- to 15.22-fold) than **29b**, indicating that increasing the
43
44 number of N atoms at the R-position is not effective to improve the activity of
45
46 oseltamivir derivatives.
47
48
49
50
51

52 Collectively, apart from the identified group-1 NAs-selective inhibitors (**29a** and
53
54 **29b**), the NA-inhibitory activities of the novel oseltamivir derivatives are very
55
56
57
58
59
60

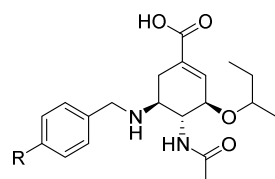
1
2
3 sensitive to the size, flexibility, and hydrophobicity of the R group. Indeed, **15b** and
4
5
6 **15c** with R groups of moderate size, flexibility, and hydrophobicity proved to be the
7
8 most potent NA inhibitors and exhibited increased inhibitory activities towards the
9
10 whole panel of wild-type NAs, especially the group-2 NAs. Our results indicate that
11
12 *N,N*-diethylamino and 1-pyrrolidine groups bound well with the 150-cavity of
13
14 group-1 NAs, and that they are likely to induce opening of the 150-loop of 09N1 and
15
16 group-2 NAs, while other structural parts interact with the active site in a similar
17
18 manner to the case of OSC.
19
20
21

22
23 As for NA of the H5N1-H274Y mutant virus, which has been reported to be
24
25 oseltamivir-resistant,^{34,44,45} OSC showed sharply reduced potency ($IC_{50} = 1630$ nM),
26
27 which was approximately 50-fold lower than that towards the wild-type NA of H5N1
28
29 ($IC_{50} = 33.56$ nM); this result is in agreement with the finding of Schade and Xie.^{34,44}
30
31

32
33 Among these oseltamivir derivatives, nine were found to be less active or to lack
34
35 activity at the highest tested concentration of 100 μ M against the mutant
36
37 H5N1-H274Y NA. However, it is noteworthy that compounds **15b** and **15c** displayed
38
39 superior activity ($IC_{50} = 387.07$ and 663.9 nM, respectively), being 4- and 2-fold more
40
41 potent than OSC, respectively. Besides, two representative compounds **15b** and **15c**
42
43 were also performed an enzymatic assay against NA of H3N2-E119V, and the results
44
45 are shown in Table 2. The NA of H3N2-E119V confer resistance to oseltamivir
46
47 without altering susceptibility to zanamivir, which is consistent with reported data.⁴⁶
48
49

50
51 **15b** and **15c** displayed robust potencies against NA of H3N2-E119V, with IC_{50} values
52
53 of 603.83 and 288.5 nM, respectively, which were more potent than OSC. These
54
55
56

1
2
3 compounds could serve as suitable lead compounds for further optimization studies
4
5
6
7
8
9
10
11
12
13
14
15
16
17
18
19
20
21
22
23
24
25
26
27
28
29
30
31
32
33
34
35
36
37
38
39
40
41
42
43
44
45
46
47
48
49
50
51
52
53
54
55
56
57
58
59
60

Table 1. Neuraminidase (NA) Inhibition of Oseltamivir Derivatives in Chemiluminescence-based Assay

Compound	R	NA Enzyme-Inhibitory Assay, IC ₅₀ (nM) ^a									
		H1N1 ^b	H1N1pdm09 ^c	H3N2 ^d	H5N1 ^e	H5N2 ^f	H5N6 ^g	H5N8 ^h	H9N2 ⁱ	H7N9 ^j	H5N1-H274Y ^k
		group-1	group-1	group-2	group-1	group-2	group-2	group-1	group-2	group-2	group-1
15a		5.06±0.04	4.09±0.13	4.11±0.13	120.93±14.59	8.89±0.43	33.85±4.48	9.53±0.56	5.74±0.61	8.41±0.74	3365.67±181.95
15b		1.16±0.01	0.55±0.03	1.05±0.01	33.72±2.95	0.49±0.06	1.26±0.08	5.34±0.67	0.35±0.003	1.79±0.17	387.07±16.46
15c		2.65±0.09	2.31±0.03	1.81±0.07	14.31±1.80	4.50±0.09	10.85±0.73	4.06±0.38	2.13±0.08	6.51±0.12	663.9±98.31
15d		24.92±0.20	18.61±0.68	17.15±0.83	165.90±16.09	16.64±0.77	73.82±18.22	57.46±3.01	20.74±0.12	40.46±3.83	10028.33±679.75
19		65.93±1.82	48.38±1.54	62.59±4.55	557.77±60.10	127.63±10.79	363.57±37.51	288.37±24.70	74.18±3.22	155.90±14.72	>100000 ^l
22		17.49±1.96	17.31±0.17	10.91±0.47	581.03±34.54	31.73±6.92	181.17±21.68	216.53±23.56	13.66±0.30	31.47±0.18	9387±717.29
26a		73.48±13.87	66.72±0.83	31.12±0.83	599.17±20.71	138.23±13.11	539.03±54.17	368.70±42.86	27.39±1.47	94.20±6.08	12540±1126.41

26b		9.62±0.98	29.82±0.34	5.65±0.29	454.67±57.07	62.84±8.02	224.87±12.47	29.00±3.41	2.29±0.04	11.37±0.54	1485.67±168.84
26c		361.67±24.80	697.77±57.33	473.73±31.78	275.30±20.54	1558.33±198.56	24803.33±5028.49	817.37±21.47	559.63±24.45	2586±0.29	38083.33±2.46.62
29a		72.64±4.08	59.34±1.96	327.23±37.86	38.11±3.33	192.6±52.08	1038.8±222.30	43.89±5.57	504.10±31.13	1820.67±95.52	5007±242.19
29b		374.43±24.66	297±27.34	869.30±115.28	266.97±39.42	2923.67±499.44	1322±156.69	360.70±30.71	592.80±59.80	9123.33±968.92	46686.67±7085.37
6 ⁿ		22.63±1.27	21.27±0.28	353.50±35.68	9.79±0.09	389.10±28.76	6870±1438.31	17.87±2.85	163.57±9.58	1463.33±112.33	160±20. ^m
OSC		5.39±0.47	4.45±0.12	7.14±0.29	33.56±3.40	5.40±0.49	15.72±2.69	7.77±1.46	4.17±0.15	8.42±0.68	1630±41.87
zanamivir ^o		5.31±0.19	4.32±0.09	6.82±0.25	9.81±0.56	13.01±0.59	22.80±1.08	7.39±0.92	9.15±0.45	17.61±0.43	6.71±1.17

^a Concentration required to reduce NA activity to 50% of control NA activity (IC₅₀). Values are the mean of three experiments, presented as the mean ± standard deviation (SD). ^b A/PuertoRico/8/1934. ^c A/California/04/2009. ^d A/Babool/36/2005. ^e A/goose/Guangdong/SH7/2013. ^f A/Chicken/Hebei/LZF/2014. ^g A/duck/Guangdong/674/2014. ^h A/goose/Jiangsu/1306/2014. ⁱ A/chicken/china/415/2013. ^j A/Anhui/1/2013. ^k A/Anhui/1/2005. ^l Highest tested concentration. ^m Xie *Y. J. Med. Chem.* **2014**, *57*, 8445–8458. ⁿ Lead compound (originally numbered **32**, *J. Med. Chem.* **2014**, *57*, 8445-8458). ^o Zanamivir was found to be more potent towards group-1 NAs (with IC₅₀ values of 4.32-9.81 nM) than towards group-2 NAs (with IC₅₀ values of 6.82-22.80 nM). In agreement with the results of a previous study,⁴⁷ zanamivir is more potent than OSC towards group-1 NAs but less potent than OSC towards group-2 NAs. The inhibitory effect of zanamivir on the

1
2
3
4
5
6
7
8
9
10
11
12
13
14
15
16
17
18
19
20
21
22
23
24
25
26
27
28
29
30
31
32
33
34
35
36
37
38
39
40
41
42
43
44
45
46
47

NA (H5N1-H274Y) ($IC_{50} = 6.71 \text{ nM}$) is still at a very effective level.

Table 2. N2 (H3N2-E119V) Inhibitory Activities of Compounds 15b and 15c^a

compounds	15b	15c	OSC	zanamivir
N2 (H3N2-E119V) ^b (nM)	603.83±32.39	288.5±26.18	817.43±98.61	33.55±1.99

^a Values are the mean of three independent experiments. ^b A/Babol/36/2005 (H3N2)

Anti-Influenza-Virus Activity in Cell Culture

In order to investigate the efficacy of target compounds against influenza virus infection, we examined all the synthesized NAIs in cell-based assays that address the cytopathic effect (CPE) of AIV infection, using A/goose/Guangdong/SH7/2013 (H5N1) and A/goose/Jiangsu/1306/2014 (H5N8), as models for group-1 NAs-containing influenza strains, and A/Chicken/Hebei/LZF/2014 (H5N2), A/duck/Guangdong/674/2014 (H5N6) as models for group-2 NAs-containing influenza strains. As in the enzyme inhibition assay, OSC, zanamivir, and **6** were used as reference compounds in parallel. The values of EC₅₀ (anti-avian influenza A virus potency) and CC₅₀ (cytotoxicity) of the synthesized compounds are summarized in Table 3. Notably, all the tested compounds exhibited no appreciable cytotoxicity at the highest tested concentrations (CC₅₀ > 200 μM) in chicken embryo fibroblasts (CEFs).

In the case of the H5N1 virus, the activities of **15a** (EC₅₀ = 0.53 μM), **15b** (EC₅₀ = 0.47 μM) and **15c** (EC₅₀ = 0.49 μM) were superior to that of OSC. In contrast, **15d**, **19**, **22**, **26a-26c**, **29a**, and **29b** displayed sharply reduced antiviral activity. In particular, **19** bearing 4-thiomorpholine (EC₅₀ = 49.72 μM) and **22** bearing acetamide substituents (EC₅₀ > 100 μM) almost lacked anti-influenza potency. Overall, the anti-H5N1 activities of the novel oseltamivir derivatives were consistent with the results of the N1 (H5N1)-inhibitory activities, with the exception of **15a**.

As for H5N2 virus, the antiviral activities of **15b** (EC₅₀ = 0.012 μM) and **15c** (EC₅₀ = 0.063 μM) were consistent with the N2 (H5N2)-inhibitory activities, and these compounds showed significantly greater activity than the reference compounds.

1
2
3 In addition, **15a**, **15d**, **22**, **29a**, and **26a-26c** exhibited EC_{50} values in the
4 submicromolar range, being inferior to OSC, in accordance with their less potent
5 inhibitory activities for NA of H5N2. Similarly, **29b** and **19** showed reduced antiviral
6 activities ($EC_{50} = 1.25$ and $1.54 \mu\text{M}$, respectively), in accordance with their N2
7 (H5N2)-inhibitory activities.
8
9

10
11
12
13
14 Against H5N6 virus, **15b** ($EC_{50} = 0.17 \mu\text{M}$) and **15c** ($EC_{50} = 0.38 \mu\text{M}$) turned out
15 to be the most potent inhibitors, being 6- and 3-fold more potent than OSC,
16 respectively. This is in line with their N6 (H5N6)-inhibitory activities. Moreover, **19**
17 also showed more potent antiviral activity ($EC_{50} = 0.49 \mu\text{M}$) than OSC. The activities
18 of **15a** ($EC_{50} = 0.86 \mu\text{M}$), **15d** ($EC_{50} = 1.60 \mu\text{M}$), **26a** ($EC_{50} = 1.07 \mu\text{M}$), **26b** ($EC_{50} =$
19 $1.78 \mu\text{M}$) and **26c** ($EC_{50} = 0.74 \mu\text{M}$) were equivalent to that of OSC. Compound **22**
20 ($EC_{50} = 5.69 \mu\text{M}$), in accordance with its lack of N6 (H5N6)-inhibitory activity, was
21 ineffective against H5N6 virus. Like **6**, which showed selective anti-H5N1 and H5N8
22 virus activity, **29a** and **29b** showed 5-14 times lower anti-H5N6 potency than OSC.
23
24
25
26
27
28
29
30
31
32

33
34 More than half of the new oseltamivir derivatives in this study were found to
35 show improved anti-H5N8 virus activities in comparison with OSC and zanamivir.
36 Among them, **15a**, **15b**, **15c** and **29a** were highly potent anti-H5N8 virus agents, with
37 EC_{50} values ranging from 0.61 to $0.95 \mu\text{M}$, which are lower than those of OSC and
38 zanamivir. Compounds **29b** and **26a** showed comparable anti-H5N8 virus activities
39 relative to OSC. Interestingly, **26b** and **26c** exhibited the most potent activities, with
40 EC_{50} values of 0.29 and $0.31 \mu\text{M}$, respectively, being greatly superior to the reference
41 compounds. Although **15d** and **22** displayed moderate activity in N8 (H5N8)
42 inhibition assay, they showed attenuated anti-H5N8 virus activities with $EC_{50} = 6.78$
43 μM and $16.27 \mu\text{M}$, respectively, comparable to the reference compounds.
44
45
46
47
48
49
50
51
52
53
54
55
56
57
58
59
60
Unsurprisingly, **19**, which displayed a considerable decrease in N8 (H5N8)-inhibitory

activity, was inactive toward H5N8 virus even at the highest tested concentration of 100 μM .

Among the novel oseltamivir derivatives examined, **15b** and **15c** showed robust antiviral activity against the viral panel, being more effective than OSC in the same cellular assays; the EC_{50} values of **15b**, **15c**, and OSC were in the ranges of 0.012-0.61 μM , 0.063-0.75 μM , and 0.07-1.22 μM , respectively. More importantly, **15b** and **15c** exhibited more potent activity towards H5N2 and H5N6 than towards H5N1 and H5N8 viruses. This is consistent with their N1 (H5N1), N2 (H5N2), N6 (H5N6), and N8 (H5N8) inhibitory activities. It is also noteworthy that **26b** and **26c** showed remarkably improved anti-H5N8 virus activity in the cellular system, although they displayed only moderate N8 (H5N8)-inhibitory activities. The phenomenon that the potency of compounds can increase in a cellular environment may be due to multiple factors, including synergistic inhibition,⁴⁸ cellular metabolism, protein-protein interactions, and asymmetric intracellular localization.⁴⁹

Table 3. Anti-Influenza Virus Activity and Cytotoxicity of Oseltamivir Derivatives (CEFs)

Compound	R	EC_{50}^a values (μM) towards influenza viruses				CC_{50}^b
		H5N1	H5N2	H5N6	H5N8	
		group-1	group-2	group-2	group-1	
15a		0.53±0.28	0.17±0.05	0.86±0.11	0.95±0.64	>200 ^c
15b		0.47±0.09	0.012±0.002	0.17±0.03	0.61±0.15	>200
15c		0.49±0.02	0.063±0.02	0.38±0.13	0.75±0.21	>200
15d		3.02±0.77	0.86±0.38	1.60±0.79	6.78±1.62	>200
19		49.72±18.33	1.25±0.27	0.49±0.07	>100 ^c	>200

22		>100 ^c	0.299±0.14	5.69±2.37	16.27±4.84	>200
26a		5.11±1.43	0.17±0.06	1.07±0.16	1.16±0.06	>200
26b		13.13±1.12	0.44±0.18	1.78±0.79	0.29±0.13	>200
26c		23.54±6.88	0.57±0.12	0.74±0.14	0.31±0.13	>200
29a		2.32±0.52	0.36±0.17	14.17±5.53	0.63±0.02	>200
29b		10.94±2.67	1.54±0.26	9.26±2.19	1.99±0.44	>200
6 ^d		0.34±0.06	2.19±0.54	9.67±1.98	0.85±0.07	>200
OSC		0.63±0.07	0.07±0.03	1.05±0.18	1.22±0.20	>200
Zanamivir ^e		0.23±0.11	0.51±0.24	0.58±0.08	3.76±1.41	>200

^a EC₅₀: concentration of compound required to achieve 50% protection of CEF cell cultures against influenza virus-induced cytotoxicity, presented as the mean ± standard deviation (SD) and determined by the CCK-8 method.

^b CC₅₀: concentration required to reduce the viability of mock-infected cell cultures by 50%, as determined by the CCK-8 method.

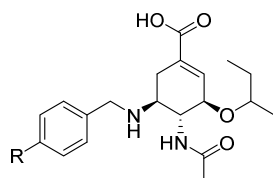
^c Highest tested concentration. ^d Lead compound **6** (originally numbered **32**, J. Med. Chem. 2014, 57, 8445-8458).

^e Zanamivir displayed antiviral activity against H5N1, H5N2 and H5N6 virus with EC₅₀ values in the submicromolar range and against H5N8 with EC₅₀ values in the micromolar range.

Then, we tested compounds **15b**, **15c**, **19**, **26b**, and **29a** in plaque reduction assays (PRA) with both the A/PR/8/34 (H1N1) and the A/Wisconsin/67/05 (H3N2) strain in MDCK cells. OSC and ZAN were used as positive controls for inhibition. We also tested the cytotoxicity of the test compounds, as well as OSC and ZAN as a reference, in MDCK cells by MTT assays. No cytotoxic effect was observed at the tested concentrations (250 μM) for any of the compounds. In the inhibitory activity evaluation against H1N1 and H3N2 strains, **15b** exhibited the greatest inhibition, with

EC₅₀ values of 0.065 and 1.70 μM, respectively, which are similar to those of OSC and ZA. **15c** had slightly decreased activity against H1N1 and H3N2 relative to OSC. However, other compounds (**19**, **26b**, and **29a**) showed remarkably reduced antiviral activity than OSC and ZA toward the two strains.

Table 4. Anti-Influenza Virus Activity and Cytotoxicity of Oseltamivir Derivatives (MDCK)



Compound	R	EC ₅₀ ^a values (μM) towards influenza viruses		CC ₅₀ ^b
		H1N1 ^c	H3N2 ^d	
		group-1	group-2	
15b		0.07 ± 0.01	1.7 ± 0.6	>250 ^e
15c		0.22 ± 0.01	2.35 ± 0.2	>250
19		4.4 ± 1.0	19.0 ± 1.0	>250
26b		1.95 ± 0.35	25.55 ± 6.7	>250
29a		0.69 ± 0.06	29.0 ± 8.9	>250
OSC		0.04 ± 0.02	0.90 ± 0.14	>250
Zanamivir		0.05 ± 0.03	0.27 ± 0.06	>250

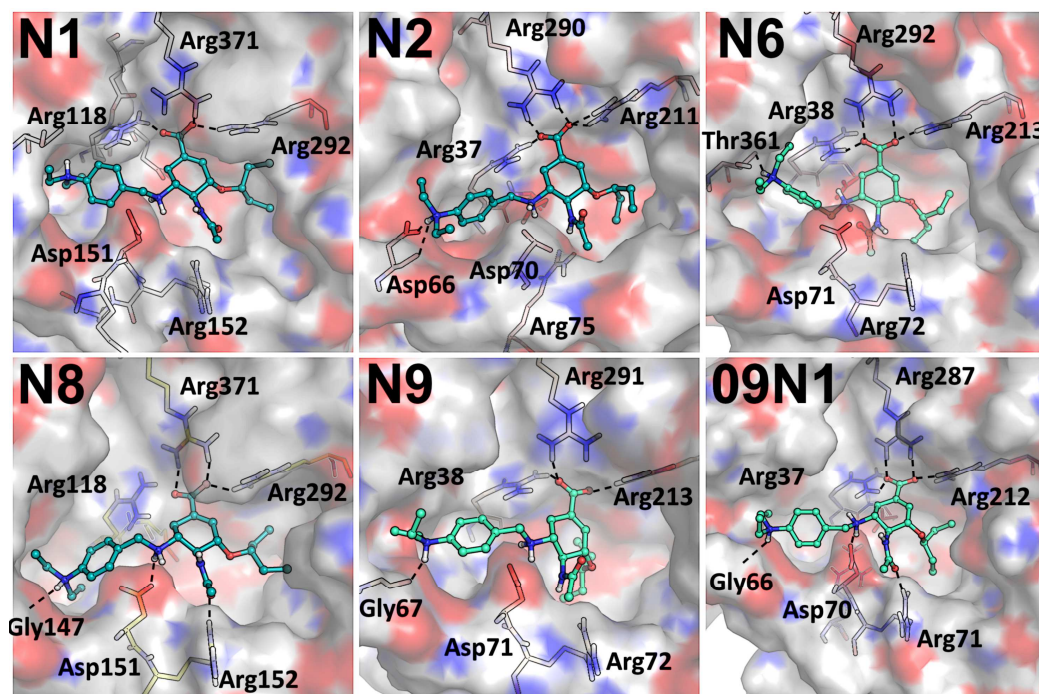
^a EC₅₀: concentration of compound required to achieve 50% protection of MDCK cell cultures against influenza virus-plaque formation, presented as the mean ± standard deviation (SD) and determined by the PRA method.

^b CC₅₀: concentration required to reduce the viability of mock-infected cell cultures by 50%, as determined by the MTT method.

^c A/PR/8/34. ^d A/Wisconsin/67/05. ^e Highest tested concentration.

MOLECULAR MODELING

To further understand and characterize the interaction pattern of the synthesized compounds with the various NAs, the most promising ligand **15b** and **OSC** were subjected to computational docking into an open 150-loop conformation of the N1, N2, N6, N8, N9 and 09N1 strains, followed by explicit solvent MD simulations. Initially, both compounds were docked into the open-form structure of each NA using the Glide program and the best protein-ligand complex (*pose*) was chosen as the starting configuration for MD simulations; i.e., 12 simulations were performed in total. Of the 20 ns production run, only trajectories from the last 5 ns (500 snapshots) were retrieved for analysis (see the method section for more information). For each complex, the 500 snapshots were analyzed with respect to energy convergence in order to ensure that the protein-ligand complex is energetically stable (Supporting information, Figure S2).



1
2
3 **Figure 5.** Snapshots showing the binding mode of **15b** (ball and stick) in the NA-binding sites.
4 Important residues are highlighted and polar interactions are indicated by dotted lines.
5
6

7 As can be seen in **Figure 5**, compound **15b** shows key interactions, such as
8 salt-bridge formation between carboxylate and Arg (N1 and N8 of Arg371, 09N1 of
9 Arg287, N2 of Arg290, N9 of Arg291, N6 of Arg292) and hydrogen bonding between
10 the acetamide group and Arg (Arg152 in N8 and Arg71 in 09N1), as observed in the
11 X-ray crystal structures of N8 bound to OSC.³⁰ Schematic representation of
12 protein-ligand interaction of **15b** and binding mode OSC is provided in Supporting
13 information, Figure S3 and Figure S4, respectively. The 5-amino linker in the
14 molecule was also involved in hydrogen bonding with Asp located between the active
15 site and the 150-cavity; this interaction is unique to **15b**, and no such interaction was
16 observed when the 5-amino group of OSC was unsubstituted. As described in the
17 design section, N-substituted groups such as polar groups or aromatic rings may
18 induce the open 150-cavity conformation, and may thereby increase the overall
19 binding affinity. The MD simulation results indicate that *N,N*-diethylamino group of
20 **15b** strongly binds to the 150-cavity of all six NAs. In particular, the aromatic ring is
21 solely surrounded by non-polar residues (Val, Thr and Pro) and the amino group in the
22 *N,N*-diethylamino fragment is hydrogen-bonded with either Gly (147 of N8, 67 of N9,
23 66 of 09N1) or Thr (361 of N6) or Asp (66 of N2) in the 150-cavity. All of these
24 interactions result in a high degree of structural complementarity.
25
26
27
28
29
30
31
32
33
34
35
36
37
38
39
40
41
42
43
44
45

46 Also, to further assess which part of the protein shows high flexibility during
47 MD simulations when **15b** and OSC are bound to NAs, we calculated the RMSF (root
48 mean square fluctuation) and B-factor. The calculated B-factors were compared to the
49 X-ray crystal structure values (the B-factor and average RMSF of protein atoms as a
50 function of residue number are provided in the Supporting Information, Figure S5).
51
52
53
54
55
56
57
58
59
60

1
2
3 This information is essential to understand whether or not a ligand especially
4 stabilizes the ligand-binding pocket (150-cavity) when bound to NAs. The **B**-factor
5 values suggest that there is high mobility in the crystal structure, particularly at the
6 150-loop region, in all six NAs. In accordance with this, MD simulation with OSC
7 showed high flexibility in the 150-loop region in all six NA simulations. Interestingly,
8 when compound **15b** is bound at the active site, the overall flexibility of the 150-loop
9 is significantly reduced, which clearly indicates that the *N,N*-diethylamino group in
10 **15b** strongly stabilizes the 150-cavity through non-bonded interactions, for instance,
11 hydrogen-bonding of the *N,N*-diethylamino group with polar residues such as Gly
12 (147 of N8, 67 of N9, 66 of 09N1) or Thr (361 of N6) or Asp (66 of N2) in the
13 150-cavity.
14
15
16
17
18
19
20
21
22
23
24
25

26
27 Also, protein-ligand interaction fingerprint (PLIF) analysis was performed for
28 compounds 15b, 15c, and 15d to understand the binding mode and characterize their
29 key interactions with NAs (see PLIF analysis in the SI). Results obtained from the
30 PLIF analysis suggest that 15b-d showed similar binding mode in all six NAs, i.e.,
31 compounds binding in the both active site and 150-cavity, but only differ in the
32 position of the linker group (phenyl ring) which is passing through a small tunnel
33 located between “active site” and “150-cavity” for 15b and 15c. Due to slightly
34 bulkier piperidine ring, 15d adjusts its binding mode in a way to reduce the steric
35 hindrance with “150-cavity” and linker region lies on the top of passage to 150-cavity
36 (Figure 6) which could significantly reduce the affinity as compared to 15b or 15c (cf.
37 PLIF section in Supporting Information). To further improve the binding affinity of
38 molecule 15b without adding a bulky group in the N-substituted side chain position,
39 substitution at phenyl ring (linker) either at *meta* or *ortho* position pay way for further
40 lead optimization.
41
42
43
44
45
46
47
48
49
50
51
52
53
54
55
56
57
58
59
60

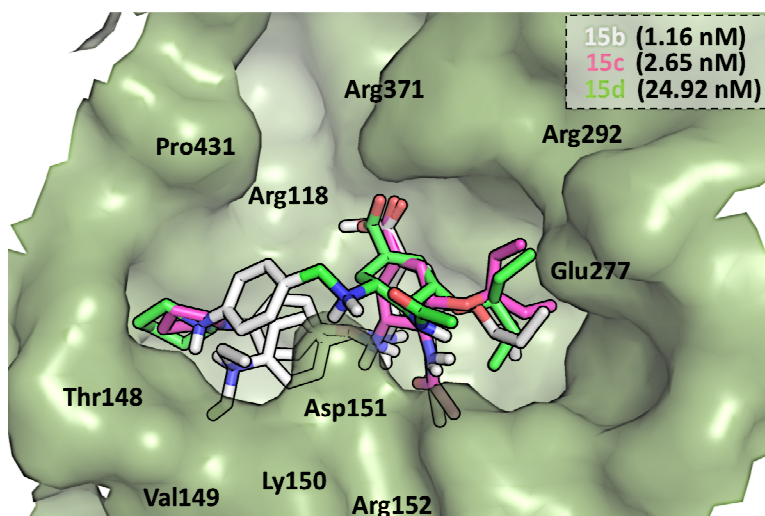


Figure 6. Binding modes of 15b (white), 15c (red), and 15d (green) with the N1 crystal structure (PDB ID: 3BEQ).

Further, we compared the amino acid sequences of six NAs (A/goose/Guangdong/SH7/2013 (H5N1), A/Chicken/Hebei/LZF/2014 (H5N2), A/chicken/china/415/2013 (H9N2), A/duck/Guangdong/674/2014 (H5N6), A/goose/Jiangsu/1306/2014 (H5N8) and A/Anhui/1/2013 (H7N9)) with those of proteins of the same NA subtype (2HU0, 3NSS, 4K1I, 5HUM, and 2HT7) as used for the MD simulation studies. We found that NAs of the same subtypes showed a high degree of similarity (> 90% for N1 of H5N1, 2HU0, and 3NSS; > 88% for N2 of H5N2 and H9N2, and 4K1I; > 99% for N6 of H5N6 and 5HUM; > 93% for N8 of H5N8 and 2HT7; 100% for N9 of H7N9 and 5L15 respectively; data shown in the Supporting Information S5). No more than 50 of the nearly 400 residues are different in NAs of the same subtype, and this supports the credibility of the MD simulation studies. The MD simulation protocol is described in the MD simulation studies section.

METABOLIC STABILITY IN THE PRESENCE OF HUMAN LIVER MICROSOMES AND STABILITY IN HUMAN PLASMA

The metabolic stability of **15b** and **14b** (the ethyl carboxylate of **15b**) was measured in a human liver microsomes (HLM) assay. Testosterone, diclofenac, and propranolol were used as control compounds with moderate metabolic stability. As shown in Table 4 and Figure 7, only 0.6% of **14b** remained after incubation for 60 min. The metabolite of **14b** was confirmed to be **15b** by LC-MS/MS. In contrast, 82.7% of compound **15b** remained intact in the HLM assay, and no significant amount of metabolite was found by LC-MS/MS. Compound **15b** ($t_{1/2} > 145$ min) showed greater metabolic stability than the control compounds ($t_{1/2}$ values of 26.6 min for testosterone, 12.3 min for diclofenac, and 6.4 min for propranolol). Moreover, the intrinsic clearance (CL) of **15b** was very much lower (< 9.6 $\mu\text{L}/\text{min}/\text{mg}$) than those of control compounds in the same assay.

The stability of **15b** was also evaluated in a human plasma assay. Propantheline bromide was tested for comparison. As shown in Table 5, **15b** remained intact (measured as 120.7% of the initial amount) after incubation for 120 min, and **15b** showed much greater stability than propantheline bromide (1.8% after 120 min). In short, **15b** showed reasonable metabolic stability in HLM and good stability in human plasma. Therefore, the *N,N*-diethyl-4-methylaniline moiety at the C-5 amino group of oseltamivir seems to be a privileged modification with a drug-like profile.

Table 5. Metabolic Stability of 15b and 14b in the Presence of Human Liver Microsomes

Compound	HLM (final concentration: 0.5 mg protein/mL)					
	R^{2a}	$T_{1/2}^b$ (min)	$CL_{\text{int(mic)}}^c$ ($\mu\text{L}/\text{min}/\text{mg}$)	$CL_{\text{int(liver)}}^d$ ($\text{mL}/\text{min}/\text{kg}$)	Remaining ($T = 60$ min)	Remaining (*NCF ^e =60 min)
15b	0.7653	>145	<9.6	<8.6	82.7%	95.4%
14b	0.9592	8.4	165.2	148.7	0.6%	87.1%
Testosterone	0.9760	26.6	52.1	46.9	19.1%	78.0%

Diclofenac	0.9973	12.3	112.3	101.1	3.3%	84.5%
Propafenone	0.9680	6.4	215.9	194.3	0.2%	90.1%

^a R^2 is the correlation coefficient of the linear regression for the determination of the kinetic constant (see raw data worksheet in the Supporting Information).

^b $T_{1/2}$ is the half-life and CL_{int} (mic) is the intrinsic clearance.

^c CL_{int} (mic) = 0.693/half-life/mg microsomal protein per mL.

^d $CL_{int(liver)} = CL_{int}$ (mic) \times mg microsomal protein/g liver weight \times g liver weight/kg body weight.

^e *NCF indicates no co-factor. No NADPH-regenerating system was added to the NCF sample (replaced with buffer) during the 60-min incubation.

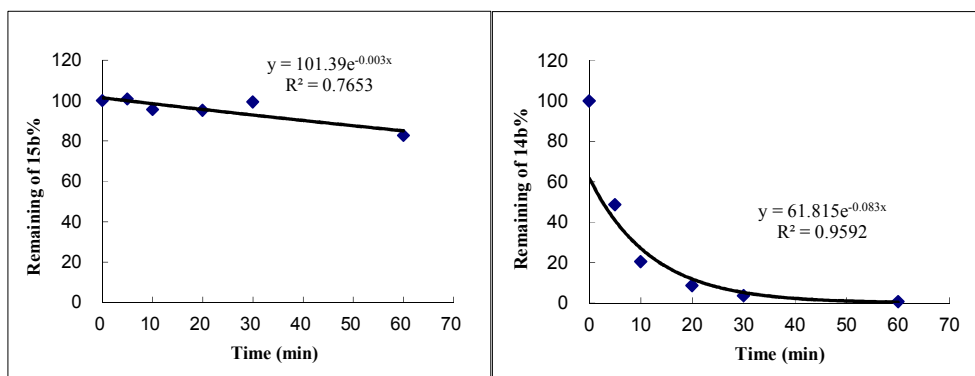


Figure 7. Metabolic stability - Time courses of remaining **15b** and **14b** in the presence of human liver microsomes.

Table 6. Summary of the Results of Plasma Stability Assay

Compound	Batch	Time Point (min)	% Remaining ^a
			Human
15b	/	0	100.0
		10	117.5
		30	119.5
		60	119.9
		120	120.7 ^b
Proprantheline bromide	110M1921V	0	100.0
		10	73.4
		30	44.6
		60	16.8

120

1.8

^a % Remaining = $100 \times (\text{PAR at appointed incubation time} / \text{PAR at T0})$ PAR is the peak area ratio of test compound versus internal standard. Accuracy should be within the range of 80%~120% of the marked value.

^b Outlier, but the analysis acceptance criteria were still met.

SAFETY ASSESSMENT

Single-dose acute toxicity was studied in mice. After intragastric administration of **15b** at a dose of 0.5 and 1 g·kg⁻¹, no death occurred, and there was no abnormality of body weight increase over the subsequent one week.

CONCLUSION

In drug discovery, slight structural modifications of the lead compound can result in dramatic changes in potency and physicochemical properties, a phenomenon that is known as an “activity cliff” in the activity landscape.^{50,51} Therefore, the elaboration of approved drugs (OSC in this research) via subsequent medicinal chemistry campaigns based on three-dimensional structure data for NA-inhibitor interactions, such as multidimensional optimization and comprehensive SAR, is still highly desirable to improve the activity and selectivity and to overcome drug resistance.

We previously focused on the open 150-cavity adjacent to the active site of influenza A viral group-1 NAs, except for 09N1, as a target for the design of novel group-1 NAs-selective inhibitors. In this work, considering that several crystal structures and in silico studies have indicated that group-2 NAs are also able to adopt an open 150-cavity under the influence of specific ligands, we aimed to discover potent group-1 and -2 NAIs through structure-based modification studies, focusing on detailed optimization of the *para*-position (R-position) of the benzyl group of

1
2
3 compound **5** or **6**. All the changes at the R-position involving relatively bulky, rigid
4 (**15d**, **19**, and **26a-26c**), small (**15a**) or amide (**22**) substituents appeared to have a
5 negative effect on potency in NAs inhibition assays. Although several compounds
6 exhibited high potency against H5N6 or H5N8 (for instance, **26b** and **26c** were
7 superior to the reference compounds against H5N8), they showed decreased activity
8 in the anti-influenza virus activity study in CEF. Like the reference compound **6**, **29a**
9 and **29b** also turned to be group-1-specific NA inhibitors.

10
11
12
13
14
15
16
17
18 On the other hand, **15b** and **15c**, with medium-sized substituents were mostly
19 superior to the reference compounds in inhibiting NAs of H1N1, H1N1pdm09, H5N1
20 and H5N8 (group-1), and H3N2, H5N2, H9N2, H5N6, and H7N9 (group-2).
21 Importantly, **15b** showed similar or greater inhibitory potency against group-2 NAs
22 and 09N1 (IC₅₀ values of 0.35-1.79 nM) compared with the activities against group-1
23 NAs (IC₅₀ values of 1.16-33.72 nM). In addition, **15b** and **15c** exhibited high
24 activities against H5N1-H274Y and H3N2-E19V mutant NA. Both of them also
25 exerted the greatest inhibition, with IC₅₀ values of 89.28 and 86.04 nM against
26 influenza B neuraminidase, respectively, which are similar to that of oseltamivir
27 carboxylate (OSC, IC₅₀ = 60.59nM) (see Supporting Information). In cellular assays
28 (CEFs) too, **15b** and **15c** again exhibited better activity than OSC against AIV (H5N1,
29 H5N2, H5N6, and H5N8), in accordance with the results of the NA-inhibitory
30 activities. Similarly, **15b** and **15c** showed more potent antiviral activities against
31 H5N2 and H5N6 viruses (containing group-2 NAs) than against H5N1 and H5N8
32 viruses (containing group-1 NAs).

33
34
35
36
37
38
39
40
41
42
43
44
45
46
47
48
49
50 Finally, the results of MD simulation studies clearly show that **15b** occupies the
51 150-cavity in addition to retaining other key interactions of OSC in the active site of
52 NAs. The molecular modeling studies also support the design hypothesis of this study,
53
54
55
56

1
2
3 i.e. that the N-substituted benzyl group would enhance the binding affinity by
4 inducing the 150-cavity next to the active site, as proposed before.²⁹ Furthermore, in
5 the stability assays, **15b** showed greater metabolic stability than all the reference
6 substances in HLM and human plasma assays.
7
8
9

10
11 On the basis of these excellent in vitro and in vivo results, we consider that **15b**
12 and **15c** are promising new drug candidates to treat influenza, and may have the
13 potential to prevent or ameliorate the next pandemic.
14
15
16
17
18
19

20 **EXPERIMENTAL SECTION**

21 **General Information on Synthesis**

22 Oseltamivir phosphate was provided by Shandong Qidu Pharmaceutical Co., Ltd.
23 Other chemicals and reagents were purchased from Aladdin, TCI, J&K, Energy
24 Chemical, and Sinopharm Chemical Reagent Co., Ltd. and were at least 97% pure. All
25 melting points were determined on a micro melting point apparatus (RY-1G, Tianjin
26 TianGuang Optical Instruments) and are uncorrected. ¹H-NMR and ¹³C-NMR spectra
27 were recorded in CD₃OD, CDCl₃ or DMSO-*d*₆ on a Bruker AV-400 spectrometer with
28 tetramethylsilane (TMS) as the internal standard. Coupling constants are given in
29 hertz, and chemical shifts are reported in δ values (ppm) from TMS; ESI-MS was
30 conducted using an API 4000 LC/MS spectrometer (Applied Biosystems, USA).
31 HRMS analysis was performed using an Agilent 6520 Q-TOF LC/MS spectrometer
32 (Agilent, Germany). All reactions were routinely monitored by thin layer
33 chromatography (TLC) on Silica Gel GF254 for TLC (Merck), and spots were
34 visualized with iodine vapor or by irradiation with UV light ($\lambda = 254$ nm). Flash
35 column chromatography was performed on columns packed with Silica Gel (200-300
36 mesh), purchased from Qingdao Haiyang Chemical Company. Solvents were purified
37
38
39
40
41
42
43
44
45
46
47
48
49
50
51
52
53
54
55
56

1
2
3 and dried by means of standard methods when necessary. Organic solutions were
4
5 dried over anhydrous sodium sulfate and concentrated with a rotary evaporator under
6
7 reduced pressure. Other reagents were obtained commercially and were used without
8
9 further purification. Target compounds purity were analyzed on a Waters e2695 HPLC
10
11 instrument and Waters 2998a detector with GOLD C18 column (5 μ m, 250 mm \times 4.6
12
13 mm). HPLC solvent conditions: methanol/water with 0.1% acetic acid 10-90%; flow
14
15 rate, 1.0 mL/min; UV detection, from 200-400 nm; temperature, ambient; injection
16
17 volume, 20 μ L. Purity of all tested compounds was >95%.
18
19
20
21

22 **General Procedure for the Synthesis of Compounds 14a-14d.** To a solution of
23
24 oseltamivir phosphate (0.82 g, 2.0 mmol) and an aldehyde (2.4 mmol, 1.2 equiv) in 30
25
26 mL ethanol and methanol (V:V = 2:1), NaBH₃CN (0.31 g, 5.0 mmol, 2.5 equiv) was
27
28 slowly added. The mixture was stirred at room temperature for 6 h. The solvent was
29
30 removed under reduced pressure, and then water (30 mL) was added. This mixture
31
32 was extracted with ethyl acetate and tetrahydrofuran (V:V = 2:1, 3 \times 30 mL), and the
33
34 organic phase was washed with saturated sodium chloride (2 \times 30 mL), dried over
35
36 anhydrous MgSO₄, and concentrated under reduced pressure to give the crude product,
37
38 which was purified by flash column chromatography to afford the corresponding
39
40 intermediate, **14a-14d**.
41
42
43

44 **Ethyl(3*R*,4*R*,5*S*)-4-acetamido-5-((4-(dimethylamino)benzyl)amino)-3-(penta**
45
46 **n-3-yloxy)cyclohex-1-ene-1-carboxylate (14a).** White powder, 63% yield, mp:
47
48 102.9-104.5°C. ¹H NMR (400 MHz, CDCl₃): δ 7.17 (d, *J* = 8.6 Hz, 2H, Ph-H), 6.78 (s,
49
50 1H, CH), 6.69 (d, *J* = 8.7 Hz, 2H, Ph-H), 4.30-4.15 (overlapped, 3H, CH₂, NH), 3.82
51
52 (d, *J* = 12.7 Hz, 1H, CH), 3.75-3.67 (m, 1H, CH), 3.64 (d, *J* = 12.7 Hz, 1H, CH), 3.35
53
54 (p, *J* = 5.7 Hz, 1H, CH), 3.15 (td, *J* = 9.3, 5.3 Hz, 1H, CH), 2.98-2.87 (m, 7H, 2CH₃,
55
56
57
58
59
60

1
2
3 CH), 2.79 (dd, $J = 17.8, 5.2$ Hz, 1H, CH), 2.25 (ddt, $J = 17.8, 8.8, 2.7$ Hz, 1H, CH),
4
5 2.10 (s, 1H, CH), 1.99 (s, 3H, CH₃), 1.55-1.46 (m, 4H, 2CH₂), 1.30 (t, $J = 7.1$ Hz, 3H,
6
7 CH₃), 0.89 (td, $J = 7.4, 3.3$ Hz, 6H, 2CH₃). ¹³C NMR (100 MHz, CDCl₃): δ 170.6,
8
9 166.5, 149.8, 137.3, 129.4, 129.0, 127.9, 112.7, 81.7, 77.3, 74.6, 60.8, 56.0, 53.3, 50.0,
10
11 40.7, 30.5, 26.1, 25.7, 23.7, 14.2, 9.4. ESI-MS: m/z 446.5 [M + H]⁺, C₂₅H₃₉N₃O₄
12
13 (445.60).
14

15
16 **Ethyl(3*R*,4*R*,5*S*)-4-acetamido-5-((4-(diethylamino)benzyl)amino)-3-(pentan-**
17
18 **3-yloxy)cyclohex-1-ene-1-carboxylate (14b).** Off-white powder, 66% yield, mp:
19
20 80.9-81.5 °C. ¹H NMR (400 MHz, CD₃OD): δ 7.10 (d, $J = 8.6$ Hz, 2H, Ph-H), 6.75 (s,
21
22 1H, CH), 6.64 (d, $J = 8.7$ Hz, 2H, Ph-H), 4.18 (q, $J = 7.1$ Hz, 2H, CH₂), 4.04 (d, $J =$
23
24 8.2 Hz, 1H, CH), 3.93 (dd, $J = 10.6, 8.6$ Hz, 1H, CH), 3.80 (d, $J = 12.6$ Hz, 1H, CH),
25
26 3.62 (d, $J = 12.6$ Hz, 1H, CH), 3.42-3.27 (overlapped, 5H, CH, 2CH₂), 2.98 (td, $J =$
27
28 10.1, 5.4 Hz, 1H, CH), 2.83 (dd, $J = 17.6, 5.2$ Hz, 1H, CH), 2.27 (ddt, $J = 17.3, 9.6,$
29
30 2.6 Hz, 1H, CH), 1.97 (s, 3H, CH₃), 1.52-1.39 (m, 4H, 2CH₂), 1.26 (t, $J = 7.1$ Hz, 3H,
31
32 CH₃), 1.08 (t, $J = 7.0$ Hz, 6H, 2CH₃), 0.85 (dt, $J = 10.7, 7.4$ Hz, 6H, 2CH₃). ¹³C NMR
33
34 (100 MHz, CD₃OD): δ 172.6, 166.1, 147.4, 137.4, 129.5, 128.4, 123.7, 112.0, 82.0,
35
36 75.4, 60.7, 53.8, 53.7, 48.7, 44.0, 28.7, 25.7, 25.2, 21.7, 13.1, 11.4, 8.5, 8.1. ESI-MS:
37
38 m/z 474.5 [M + H]⁺, C₂₇H₄₃N₃O₄ (473.66).
39
40

41
42 **Ethyl(3*R*,4*R*,5*S*)-4-acetamido-3-(pentan-3-yloxy)-5-((4-(pyrrolidin-1-yl)benz**
43
44 **yl)amino)cyclohex-1-ene-1-carboxylate (14c).** White powder, 64% yield, mp:
45
46 120.5-122.8 °C. ¹H NMR (400 MHz, DMSO-*d*₆): δ 7.80 (d, $J = 9.1$ Hz, 1H, NH), 7.07
47
48 (d, $J = 8.4$ Hz, 2H, Ph-H), 6.63 (s, 1H, CH), 6.47 (d, $J = 8.5$ Hz, 2H, Ph-H), 4.14 (q, J
49
50 = 7.0 Hz, 2H, CH₂), 3.98 (d, $J = 8.0$ Hz, 1H, NH), 3.76-3.59 (m, 2H, 2CH), 3.49 (d, J
51
52 = 12.7 Hz, 1H, CH), 3.35 (s, 4H, 2CH₂), 2.75-2.59 (m, 2H, 2CH), 2.12-1.98 (m, 1H,
53
54 CH), 1.99-1.88 (m, 4H, 2CH₂), 1.84 (s, 3H, CH₃), 1.68 (s, 1H, CH), 1.42 (tp, $J = 14.6,$
55
56
57
58
59
60

7.3 Hz, 4H, 2CH₂), 1.22 (t, *J* = 7.1 Hz, 3H, CH₃), 0.81 (dt, *J* = 15.3, 7.4 Hz, 6H, 2CH₃). ¹³C NMR (100 MHz, DMSO-*d*₆): δ 170.0, 166.3, 147.1, 138.4, 129.2, 129.1, 127.6, 111.8, 81.3, 75.7, 60.8, 54.6, 54.5, 50.0, 30.9, 26.0, 25.6, 25.3, 23.4, 14.5, 9.9, 9.4. ESI-MS: *m/z* 472.4 [M + H]⁺, C₂₇H₄₁N₃O₄ (471.64).

Ethyl(3*R*,4*R*,5*S*)-4-acetamido-3-(pentan-3-yloxy)-5-((4-(piperidin-1-yl)benzylamino)cyclohex-1-ene-1-carboxylate (14d). White powder, 61% yield, mp: 119.2-120.8°C. ¹H NMR (400 MHz, CD₃OD): δ 7.17 (d, *J* = 8.6 Hz, 2H, Ph-H), 6.93 (d, *J* = 8.7 Hz, 2H, Ph-H), 6.76 (s, 1H, CH), 4.20 (q, *J* = 7.1 Hz, 2H, CH₂), 4.04 (d, *J* = 8.7 Hz, 1H, CH), 3.90 (dd, *J* = 10.4, 8.5 Hz, 1H, CH), 3.76 (d, *J* = 12.6 Hz, 1H, CH), 3.59 (d, *J* = 12.6 Hz, 1H, CH), 3.36 (p, *J* = 5.6 Hz, 1H, CH), 3.14-3.05 (m, 4H, 2CH₂), 2.93-2.85 (m, 1H, CH), 2.85-2.77 (m, 1H, CH), 2.22 (ddt, *J* = 17.3, 9.4, 2.9 Hz, 1H, CH), 1.99 (s, 3H, CH₃), 1.70 (p, *J* = 5.7 Hz, 4H, 2CH₂), 1.61-1.55 (m, 2H, CH₂), 1.55-1.46 (m, 4H, 2CH₂), 1.29 (t, *J* = 7.1 Hz, 3H, CH₃), 0.89 (dt, *J* = 10.6, 7.4 Hz, 6H, 2CH₃). ¹³C NMR (100 MHz, CD₃OD): δ 172.4, 166.4, 151.5, 137.4, 130.5, 128.9, 128.7, 116.9, 82.0, 75.6, 60.6, 54.4, 53.9, 51.0, 49.0, 29.6, 25.7, 25.4, 25.3, 23.9, 21.7, 13.1, 8.5, 8.1. ESI-MS: *m/z* 486.6 [M + H]⁺, C₂₈H₄₃N₃O₄ (485.67).

Synthesis of Compounds 15a-15d. To a solution of intermediates **14a-14d** (0.8 mmol) in 20 mL of CH₃OH was added 8 mL of NaOH aqueous solution (15%). The reaction mixture was stirred at room temperature for 5-6 h. After the reaction was complete, the organic solvent was removed under reduced pressure. The residue was taken up in water (30 mL), and the pH was adjusted to 4-5 with HCl aqueous solution (2 mol/L). This solution was extracted with ethyl acetate and tetrahydrofuran (V:V = 2:1, 4 × 30 mL). The combined organic phase was washed with saturated sodium chloride (2 × 30 mL) and water (30 mL), then dried over anhydrous MgSO₄ and concentrated under reduced pressure to afford the target compounds **15a-15d**.

1
2
3 **(3R,4R,5S)-4-Acetamido-5-((4-(dimethylamino)benzyl)amino)-3-(pentan-3-yloxy)cyclohex-1-ene-1-carboxylic acid (15a)**. Pale yellow powder, 67% yield, mp: 4
5 136.1-138.5°C. ¹H NMR (400 MHz, DMSO-*d*₆): δ 8.09 (d, *J* = 6.5 Hz, 2H, NH), 7.28
6 (d, *J* = 7.9 Hz, 2H, Ph-H), 6.72 (d, *J* = 8.1 Hz, 2H, Ph-H), 6.62 (s, 1H, CH), 4.27-4.11
7 (m, 1H, CH), 4.05-3.86 (overlapped, 3H, CH, CH₂), 3.29-2.99 (overlapped, 2H, 2CH),
8 2.86 (s, 6H, 2CH₃), 2.84-2.75 (m, 1H, CH), 1.91 (overlapped, 4H, CH₃, CH),
9 1.50-1.30 (m, 4H, 2CH₂), 0.81 (dt, *J* = 17.9, 7.1 Hz, 6H, 2CH₃). ¹³C NMR (100 MHz,
10 DMSO-*d*₆): δ 170.9, 167.4, 150.8, 137.7, 131.0, 128.5, 112.5, 81.4, 75.2, 54.0, 51.7,
11 46.6, 40.6, 26.0, 25.4, 23.8, 9.8, 9.3. HRMS calcd for C₂₃H₃₅N₃O₄ [M + H]⁺:
12 418.2700. Found: *m/z* 418.2696. HPLC purity: 98.12% (263 nm).
13
14
15
16
17
18
19
20
21
22
23

24 **(3R,4R,5S)-4-Acetamido-5-((4-(diethylamino)benzyl)amino)-3-(pentan-3-yloxy)cyclohex-1-ene-1-carboxylic acid (15b)**. White powder, 71% yield, mp: 25
26 205.2-208.9°C. ¹H NMR (400 MHz, CD₃OD): δ 7.28 (d, *J* = 8.6 Hz, 2H, Ph-H), 6.79
27 (s, 1H, CH), 6.74 (d, *J* = 8.7 Hz, 2H, Ph-H), 4.26 (d, *J* = 12.9 Hz, 1H, CH), 4.24-4.14
28 (m, 2H, CH₂), 4.11 (d, *J* = 13.0 Hz, 1H, CH), 3.50 (dd, *J* = 12.3, 7.0 Hz, 1H, CH),
29 3.46 (d, *J* = 5.6 Hz, 1H, CH), 3.41 (q, *J* = 6.8 Hz, 4H, 2CH₂), 3.05 (dd, *J* = 17.1, 4.6
30 Hz, 1H, CH), 2.63 (dd, *J* = 16.9, 9.9 Hz, 1H, CH), 2.07 (s, 3H, CH₃), 1.55 (dt, *J* =
31 11.1, 5.9 Hz, 4H, 2CH₂), 1.19-1.13 (m, 6H, 2CH₃), 0.92 (q, *J* = 7.3 Hz, 6H, 2CH₃).
32 ¹³C NMR (100 MHz, CD₃OD): δ 173.4, 148.5, 134.9, 130.8, 129.4, 116.0, 112.3,
33 111.5, 82.1, 74.8, 54.2, 51.6, 44.5, 43.9, 26.5, 25.7, 25.2, 21.9, 21.6, 11.3, 8.4, 8.1.
34 HRMS calcd for C₂₅H₃₉N₃O₄ [M + H]⁺: 445.2941, Found: *m/z* 445.2944. HPLC
35 purity: 98.62% (270 nm).
36
37
38
39
40
41
42
43
44
45
46
47
48
49

50 **(3R,4R,5S)-4-Acetamido-3-(pentan-3-yloxy)-5-((4-(pyrrolidin-1-yl)benzyl)amino)cyclohex-1-ene-1-carboxylic acid (15c)**. White powder, 66% yield, mp: 51
52 168.1-170.3°C. ¹H NMR (400 MHz, DMSO-*d*₆): δ 8.12 (d, *J* = 8.9 Hz, 1H, NH), 7.30
53
54
55
56
57
58
59
60

(d, $J = 8.4$ Hz, 2H, Ph-H), 6.63 (s, 1H, CH), 6.54 (d, $J = 8.5$ Hz, 2H, Ph-H), 4.20 (d, $J = 7.3$ Hz, 1H, CH), 4.08 (d, $J = 13.0$ Hz, 1H, CH), 4.03-3.90 (m, 2H, CH₂), 3.35-3.04 (overlapped, 6H, 2CH₂, CH, CH), 2.92-2.81 (m, 1H, CH), 2.71-2.53 (m, 1H, CH), 2.19-1.74 (overlapped, 7H, 2CH₂, CH₃, CH), 1.50-1.30 (m, 4H, 2CH₂), 0.81 (dt, $J = 18.9, 7.3$ Hz, 6H, 2CH₃). ¹³C NMR (100 MHz, DMSO-*d*₆): δ 171.1, 167.2, 148.3, 138.0, 131.5, 128.1, 117.9, 111.9, 81.5, 74.9, 53.6, 51.2, 47.7, 46.2, 40.6, 26.2, 26.0, 25.4, 25.4, 23.9, 9.8, 9.3. HRMS calcd for C₂₅H₃₇N₃O₄ [M + H]⁺: 443.2784, Found: *m/z* 443.2786. HPLC purity: 96.11% (269 nm).

(3*R*,4*R*,5*S*)-4-Acetamido-3-(pentan-3-yloxy)-5-((4-(piperidin-1-yl)benzyl)amino)cyclohex-1-ene-1-carboxylic acid (15d). White powder, 67% yield, mp: 210.2-213.1°C. ¹H NMR (400 MHz, CD₃OD): δ 7.42 (d, $J = 8.0$ Hz, 2H, Ph-H), 7.09 (d, $J = 8.0$ Hz, 2H, Ph-H), 6.91 (s, 1H, CH), 4.35 (t, $J = 11.8$ Hz, 2H, CH₂), 4.25 (t, $J = 13.7$ Hz, 2H, CH₂), 3.61 (s, 1H, CH), 3.53 (s, 1H, CH), 3.33-3.26 (m, 4H), 3.12 (s, 1H, CH), 2.71 (s, 1H, CH), 2.15 (s, 3H, CH₃), 1.83-1.74 (m, 4H, 2CH₂), 1.73-1.68 (m, 2H, CH₂), 1.67-1.54 (m, 4H, 2CH₂), 1.00 (q, $J = 7.2$ Hz, 6H, 2CH₃). ¹³C NMR (100 MHz, CD₃OD): δ 157.1, 152.7, 138.7, 136.5, 130.5, 129.5, 120.0, 116.0, 82.2, 74.6, 54.4, 51.6, 49.7, 47.2, 29.5, 25.7, 25.2, 23.9, 22.0, 21.6, 8.4, 8.1. HRMS calcd for C₂₆H₃₉N₃O₄, [M + H]⁺: 457.2935, Found: *m/z* 457.2934. HPLC purity: 99.04% (256 nm).

4-Thiomorpholinobenzaldehyde (17). Thiomorpholine (2.06 g, 20 mmol) and 4-fluorobenzaldehyde (2.98 g, 24 mmol) were added to DMSO (30 mL) and K₂CO₃ (10 g, 72 mmol), and the mixture was heated at 100-120°C for 6 hours, then poured into water, and extracted with ethyl acetate. The ethyl acetate solution was washed with saturated sodium chloride (2 × 30 mL) and water (30 mL), then dried over

1
2
3 anhydrous MgSO₄ and concentrated to give the crude product. Purification by column
4 chromatography gave compound **17**. Pale yellow oil, 68% yield. ¹H NMR (400 MHz,
5 CD₃OD): δ 9.65 (s, 1H, CH), 7.73 (d, *J* = 9.0 Hz, 2H, Ph-H), 6.97 (d, *J* = 8.9 Hz, 2H,
6 Ph-H), 3.85 (dd, *J* = 6.2, 3.9 Hz, 4H, 2CH₂), 2.68-2.62 (m, 4H, 2CH₂). ¹³C NMR (100
7 MHz, CD₃OD): δ 190.9, 154.2, 131.9, 127.3, 126.1, 113.3, 49.9, 25.1. ESI-MS: *m/z*
8 208.2 [M + H]⁺, C₂₇H₄₁N₃O₄S (207.29).

9
10
11
12
13
14
15
16 **Ethyl(3*R*,4*R*,5*S*)-4-acetamido-3-(pentan-3-yloxy)-5-((4-thiomorpholinobenzyl**
17
18 **D)amino)cyclohex-1-ene-1-carboxylate (18)**. The synthetic method was similar to
19 that of **14a-14d**, starting from **17**. Pale yellow sticky oil, 63% yield. ¹H NMR (400
20 MHz, CD₃OD): δ 7.19 (d, *J* = 8.5 Hz, 2H, Ph-H), 6.90 (d, *J* = 8.6 Hz, 2H, Ph-H), 6.76
21 (s, 1H, CH), 4.20 (q, *J* = 7.1 Hz, 2H, CH₂), 4.08-4.00 (m, 1H, CH), 3.95-3.86 (m, 1H,
22 CH), 3.77 (d, *J* = 12.6 Hz, 1H, CH), 3.72 (t, *J* = 6.6 Hz, 1H, CH), 3.62-3.57 (m, 1H,
23 CH), 3.5-3.45 (m, 3H, CH₃), 3.37 (p, *J* = 5.4 Hz, 1H, CH), 2.95-2.74 (m, 2H, CH₂),
24 (s, 1H, CH), 2.75-2.63 (m, 3H, CH₃), 2.28-2.14 (m, 1H, CH), 1.99 (s, 3H, CH₃), 1.91-1.80 (m, 1H,
25 CH), 1.50 (qd, *J* = 8.7, 7.4, 5.0 Hz, 4H, 2CH₂), 1.29 (t, *J* = 7.1 Hz, 3H, CH₃), 0.89 (dt,
26 *J* = 10.6, 7.4 Hz, 6H, 2CH₃). ¹³C NMR (100 MHz, CD₃OD): δ 172.4, 166.4, 150.7,
27 137.4, 130.4, 129.0, 128.8, 117.0, 82.0, 75.6, 67.4, 60.6, 54.4, 53.9, 52.1, 48.9, 29.5,
28 26.1, 25.7, 25.3, 25.1, 21.7, 13.1, 8.5, 8.1. ESI-MS: *m/z* 504.5 [M + H]⁺,
29 C₂₇H₄₁N₃O₄S (503.70).

30
31
32
33
34
35
36
37
38
39
40
41
42
43
44 **(3*R*,4*R*,5*S*)-4-Acetamido-3-(pentan-3-yloxy)-5-((4-thiomorpholinobenzyl)ami**
45 **no)cyclohex-1-ene-1-carboxylic acid (19)**. The synthetic method was similar to that
46 of **15a-15d**, starting from **18**. White or almost white powder, 60% yield, mp:
47 165.4-167.5 °C. ¹H NMR (400 MHz, CD₃OD): δ 7.34 (d, *J* = 8.7 Hz, 2H, Ph-H), 6.97
48 (d, *J* = 8.7 Hz, 2H, Ph-H), 6.85 (s, 1H, CH), 4.25 (dd, *J* = 18.0, 10.4 Hz, 2H, CH₂),
49 4.20-4.12 (m, 2H, CH₂), 3.68-3.58 (m, 4H, 2CH₂), 3.55 (dt, *J* = 10.1, 5.0 Hz, 1H, CH),
50
51
52
53
54
55
56
57
58
59
60

1
2
3 3.44 (p, $J = 5.6$ Hz, 1H, CH), 3.05-2.96 (m, 1H, CH), 2.75-2.53 (overlapped, 5H,
4 2CH₂, CH), 2.05 (s, 3H, CH₃), 1.60-1.45 (m 4H, 2CH₂), 0.90 (q, $J = 7.5$ Hz, 6H,
5 2CH₃). ¹³C NMR (100 MHz, CD₃OD): δ 173.4, 151.6, 136.8, 131.0, 130.8, 120.1,
6 116.1, 115.8, 99.9, 82.3, 74.5, 54.4, 51.5, 51.0, 48.2, 25.9, 25.7, 25.4, 25.2, 22.0, 8.4,
7 8.1. HRMS calcd for C₂₅H₃₇N₃O₄S [M + H]⁺: 476.2577, Found: m/z 476.2578. HPLC
8
9
10
11
12
13
14
15
16
17
18
19
20
21
22
23
24
25
26
27
28
29
30
31
32
33
34
35
36
37
38
39
40
41
42
43
44
45
46
47
48
49
50
51
52
53
54
55
56
57
58
59
60

**Ethyl(3*R*,4*R*,5*S*)-4-acetamido-5-((4-acetamidobenzyl)amino)-3-(pentan-3-yl-
oxy)cyclohex-1-ene-1-carboxylate (21).** The synthetic method was similar to that of
14a-14d, starting from **20**. White powder, 76% yield, mp: 89.1-92.3°C. ¹H NMR (400
MHz, CD₃OD): δ 7.63 (d, $J = 8.5$ Hz, 2H, Ph-H), 7.40 (d, $J = 8.5$ Hz, 2H, Ph-H), 6.85
(s, 1H, CH), 4.32-4.21 (overlapped, 3H, CH₂, CH), 4.16 (d, $J = 5.1$ Hz, 2H, CH₂),
4.14-4.10 (m, 1H, CH), 3.45 (tt, $J = 11.2, 5.7$ Hz, 2H, CH₂), 3.00 (dd, $J = 17.4, 5.5$ Hz,
1H, CH), 2.64-2.52 (m, 1H, CH), 2.12 (s, 3H, CH₃), 2.03 (s, 3H, CH₃), 1.59-1.45 (m,
4H, 2CH₂), 1.30 (t, $J = 7.1$ Hz, 3H, CH₃), 0.90 (q, $J = 7.6$ Hz, 6H, 2CH₃). ¹³C NMR
(100 MHz, CD₃OD): δ 173.3, 170.4, 165.5, 139.6, 137.1, 129.9, 127.2, 127.0, 120.0,
82.3, 74.4, 60.9, 54.6, 51.8, 26.3, 25.7, 25.2, 22.4, 21.9, 21.6, 13.1, 8.4, 8.1. ESI-MS:
m/z 460.5 [M + H]⁺, C₂₅H₃₇N₃O₅ (459.59).

**(3*R*,4*R*,5*S*)-4-Acetamido-5-((4-acetamidobenzyl)amino)-3-(pentan-3-yl-
oxy)cyclohex-1-ene-1-carboxylic acid (22).** The synthetic method was similar to that of
15a-15d, and starting from **21**. White or almost white powder, 74% yield, mp:
190.9-192.5°C. ¹H NMR (400 MHz, CD₃OD): δ 7.64 (d, $J = 8.3$ Hz, 2H, Ph-H), 7.42
(d, $J = 8.3$ Hz, 2H, Ph-H), 6.77 (s, 1H, CH), 4.31 (d, $J = 13.0$ Hz, 1H, CH), 4.16
(overlapped, 3H, CH₂, CH), 3.45 (dq, $J = 16.4, 5.0$ Hz, 2H, CH₂), 3.08-2.87 (m, 1H,
CH), 2.71-2.51 (m, 1H, CH), 2.12 (s, 3H, CH₃), 2.04 (s, 3H, CH₃), 1.53 (dt, $J = 11.3,$
6.0 Hz, 4H, 2CH₂), 0.89 (q, $J = 7.5$ Hz, 6H, 2CH₃). ¹³C NMR (100 MHz, CD₃OD): δ

1
2
3 173.3, 170.4, 169.1, 139.7, 135.3, 130.1, 129.3, 126.5, 120.0, 82.1, 74.7, 54.7, 51.7,
4
5 47.2, 26.5, 25.7, 25.1, 22.4, 21.9, 8.4, 8.1. HRMS calcd for C₂₃H₃₃N₃O₅ [M + H]⁺:
6
7 432.2493. Found: m/z 432.2497. HPLC purity: 96.72% (246 nm).
8

9 **Synthesis of Aldehydes 24a-24c.** Aniline or N-methyl- or ethyl-substituted
10 aniline (20 mmol) and 4-bromobenzaldehyde (24 mmol) were added to a solution of
11 toluene (50 mL) containing Pd(OAc)₂ (56.13 mg, 0.25 mmol), BINAP (155.67 mg,
12 0.25 mmol), and Cs₂CO₃ (10 g, 30 mmol). The mixture was heated at reflux under a
13 nitrogen atmosphere for 12 h, then poured into water and extracted with ethyl acetate.
14 The organic layer was washed with saturated sodium chloride (2 × 30 mL) and water
15 (30 mL). The combined extract was dried over anhydrous MgSO₄ and concentrated
16 under reduced pressure to give the crude product. Purification by column
17 chromatography gave the corresponding product, **24a-24c**.
18
19

20 **4-(Phenylamino)benzaldehyde (24a).** Yellow crystal powder, 63% yield, mp:
21 86.5-91.2 °C. ¹H NMR (400 MHz, DMSO-*d*₆): δ 9.72 (s, 1H, CH), 8.99 (s, 1H, NH),
22 7.73 (d, *J* = 8.7 Hz, 2H, Ph-H), 7.40-7.31 (m, 2H, Ph-H), 7.23 (d, *J* = 8.5 Hz, 2H,
23 Ph-H), 7.12 (d, *J* = 8.7 Hz, 2H, Ph-H), 7.04 (t, *J* = 7.3 Hz, 1H, Ph-H). ¹³C NMR (100
24 MHz, DMSO-*d*₆): δ 190.5, 150.4, 141.2, 132.3, 129.8, 127.8, 123.0, 120.5, 114.4.
25 ESI-MS: m/z 198.3 [M + H]⁺, C₁₃H₁₁NO (197.24).
26
27

28 **4-(Methyl(phenyl)amino)benzaldehyde (24b).** Pale yellow oil, 65% yield. ¹H
29 NMR (400 MHz, DMSO-*d*₆): δ 9.72 (s, 1H, NH), 7.73-7.66 (m, 2H, Ph-H), 7.51-7.44
30 (m, 2H, Ph-H), 7.32-7.26 (m, 3H, Ph-H), 6.85-6.80 (m, 2H, Ph-H), 3.36 (s, 3H, CH₃).
31 ¹³C NMR (100 MHz, DMSO-*d*₆): δ 190.6, 153.8, 147.0, 131.8, 130.4, 126.7, 126.6,
32 126.4, 113.8, 40.6. ESI-MS: m/z 212.3 [M + H]⁺, C₁₄H₁₃NO (211.26).
33
34

35 **4-(Ethyl(phenyl)amino)benzaldehyde (24c).** Pale yellow oil, 68% yield. ¹H
36 NMR (400 MHz, DMSO-*d*₆): δ 9.69 (s, 1H, CH), 7.70-7.63 (m, 2H, Ph-H), 7.53-7.46
37
38
39
40
41
42
43
44
45
46
47
48
49
50
51
52

(m, 2H, Ph-H), 7.35-7.30 (m, 1H, Ph-H), 7.29-7.24 (m, 2H, Ph-H), 6.78-6.72 (m, 2H, Ph-H), 3.82 (q, $J = 7.1$ Hz, 2H, CH₂), 1.17 (t, $J = 7.1$ Hz, 3H, CH₃). ¹³C NMR (100 MHz, DMSO-*d*₆): δ 190.4, 153.0, 145.4, 132.0, 130.6, 127.7, 126.8, 126.4, 113.6, 46.8, 12.6. ESI-MS: m/z 226.3 [M + H]⁺, C₁₅H₁₅NO (225.29).

Synthesis of Compounds 25a-25c. The synthetic method was similar to that of **13-19**, starting from **24a-24c**.

Ethyl(3*R*,4*R*,5*S*)-4-acetamido-3-(pentan-3-yloxy)-5-((4-(phenylamino)benzyl)amino)cyclohex-1-ene-1-carboxylate (25a). Pale yellow sticky oil, 65% yield. ¹H NMR (400 MHz, DMSO-*d*₆): δ 8.12 (s, 1H, NH), 7.85 (d, $J = 9.1$ Hz, 1H, NH), 7.27-7.13 (m, 4H, Ph-H), 7.03 (t, $J = 8.1$ Hz, 4H, Ph-H), 6.80 (t, $J = 7.3$ Hz, 1H, Ph-H), 6.65 (s, 1H, CH), 4.15 (q, $J = 7.0$ Hz, 2H, CH₂), 4.04 (d, $J = 7.8$ Hz, 1H, NH), 3.45-3.30 (m, 1H, CH), 3.84-3.69 (m, 2H, CH₂), 3.63 (d, $J = 12.5$ Hz, 1H, CH), 2.90-2.76 (m, 1H, CH), 2.69 (dd, $J = 17.5, 4.6$ Hz, 1H, CH), 2.24-2.07 (m, 1H, CH), 2.04-1.69 (overlapped, 4H, CH, CH₃), 1.43 (ddt, $J = 18.6, 14.0, 7.2$ Hz, 4H, 2CH₂), 1.23 (t, $J = 7.1$ Hz, 3H, CH₃), 0.82 (dt, $J = 15.1, 7.4$ Hz, 6H, 2CH₃). ¹³C NMR (100 MHz, DMSO-*d*₆): δ 170.2, 166.2, 144.0, 138.4, 129.5, 129.5, 129.1, 128.9, 119.8, 117.1, 116.9, 81.3, 75.6, 60.8, 54.7, 49.4, 26.0, 25.6, 23.5, 14.5, 9.9, 9.4. ESI-MS: m/z 494.5 [M + H]⁺, C₂₉H₃₉N₃O₄ (493.65).

Ethyl(3*R*,4*R*,5*S*)-4-acetamido-5-((4-(methyl(phenyl)amino)benzyl)amino)-3-(pentan-3-yloxy)cyclohex-1-ene-1-carboxylate (25b). Pale yellow sticky oil, 68% yield. ¹H NMR (400 MHz, DMSO-*d*₆): δ 7.84 (d, $J = 9.1$ Hz, 1H, NH), 7.28-7.19 (m, 4H, Ph-H), 7.00-6.92 (m, 4H, Ph-H), 6.92-6.86 (m, 1H, Ph-H), 6.65 (s, 1H, CH), 4.15 (q, $J = 7.0$ Hz, 2H, CH₂), 4.03 (d, $J = 8.0$ Hz, 1H, NH), 3.81-3.67 (m, 2H, CH₂), 3.63 (d, $J = 13.2$ Hz, 1H, CH), 3.23 (s, 3H, CH₃), 2.78 (td, $J = 9.8, 5.3$ Hz, 1H, CH), 2.67 (dd, $J = 17.5, 4.9$ Hz, 1H, CH), 2.11 (dd, $J = 17.5, 9.4$ Hz, 1H, CH), 2.03-1.55

(overlapped, 4H, CH₃, CH), 1.50-1.36 (m, 4H, 2CH₂), 1.22 (t, *J* = 7.1 Hz, 3H, CH₃), 0.82 (dt, *J* = 14.9, 7.4 Hz, 6H, 2CH₃). ¹³C NMR (100 MHz, DMSO-*d*₆): δ 170.1, 166.2, 149.1, 147.8, 138.4, 129.5, 129.4, 129.0, 121.0, 119.7, 81.3, 75.6, 60.8, 54.8, 54.2, 49.5, 46.2, 30.4, 26.0, 25.6, 23.5, 14.5, 9.9, 9.4. ESI-MS: *m/z* 508.5 [M + H]⁺, C₃₀H₄₁N₃O₄ (507.68).

Ethyl(3*R*,4*R*,5*S*)-4-acetamido-5-((4-(ethyl(phenyl)amino)benzyl)amino)-3-(pentan-3-yloxy)cyclohex-1-ene-1-carboxylate (25c). Pale yellow sticky oil, 64% yield. ¹H NMR (400 MHz, DMSO-*d*₆): δ 7.82 (d, *J* = 9.1 Hz, 1H, NH), 7.27-7.17 (m, 4H, Ph-H), 6.94 (d, *J* = 8.5 Hz, 2H, Ph-H), 6.90 (d, *J* = 7.8 Hz, 2H, Ph-H), 6.85 (t, *J* = 7.3 Hz, 1H, Ph-H), 6.65 (s, 1H, CH), 4.15 (q, *J* = 7.0 Hz, 2H, CH₂), 4.03 (d, *J* = 8.0 Hz, 1H, NH), 3.80-3.65 (overlapped, 4H, 2CH, CH₂), 3.64-3.58 (m, 1H, CH), 2.78 (td, *J* = 9.7, 5.2 Hz, 1H, CH), 2.66 (dd, *J* = 17.4, 5.0 Hz, 1H, CH), 2.09 (dd, *J* = 17.4, 9.4 Hz, 1H, CH), 1.86 (s, 4H, 2CH₂), 1.51-1.36 (m, 4H, CH, CH₃), 1.22 (t, *J* = 7.1 Hz, 3H, CH₃), 1.11 (t, *J* = 7.0 Hz, overlapped 3H, CH₃), 0.82 (dt, *J* = 14.9, 7.4 Hz, 6H, 2CH₃). ¹³C NMR (100 MHz, DMSO-*d*₆): δ 170.0, 166.3, 147.9, 146.1, 138.4, 134.6, 129.4, 129.1, 121.8, 120.6, 119.7, 81.3, 75.7, 60.8, 54.9, 54.4, 49.8, 46.2, 30.9, 26.0, 25.6, 23.5, 14.5, 12.8, 9.9, 9.4. ESI-MS: *m/z* 522.5 [M + H]⁺, C₃₁H₄₃N₃O₄ (521.70).

Synthesis of Compounds 26a-26c. The synthetic method was similar to that of **15a-15d**, starting from **25a-25c**.

(3*R*,4*R*,5*S*)-4-Acetamido-3-(pentan-3-yloxy)-5-((4-(phenylamino)benzyl)amino)cyclohex-1-ene-1-carboxylic acid (26a). White powder, 59% yield, mp: 200.2-203.5°C. ¹H NMR (400 MHz, DMSO-*d*₆): δ 8.18 (s, 1H, NH), 7.91 (d, *J* = 8.8 Hz, 1H, NH), 7.24-7.07 (m, 4H, Ph-H), 7.01-6.90 (m, 4H, Ph-H), 6.73 (t, *J* = 7.2 Hz, 1H, Ph-H), 6.52 (s, 1H, CH), 4.13-4.00 (m, 1H, CH), 3.96-3.72 (overlapped, 3H, CH, CH₂), 3.14-2.99 (m, 1H, CH), 2.78-2.62 (m, 1H, CH), 2.38-2.27 (m, 1H, CH),

1
2
3 2.16-1.54 (overlapped, 4H, CH, CH₃), 1.40-1.20 (m, 4H, 2CH₂), 0.70 (dt, *J* = 14.9, 7.3
4 Hz, 6H, 2CH₃). ¹³C NMR (100 MHz, DMSO-*d*₆): δ 170.8, 167.5, 144.0, 143.4, 137.8,
5 131.0, 129.7, 129.6, 128.6, 120.4, 117.5, 116.6, 115.6, 81.5, 75.2, 54.3, 52.1, 47.1,
6 26.0, 25.5, 23.8, 23.2, 9.8, 9.3. HRMS calcd for C₂₇H₃₅N₃O₄ [M + H]⁺: 466.2700.
7 Found: m/z 466.2705. HPLC purity: 95.92% (289 nm).
8
9
10
11
12

13
14 **(3*R*,4*R*,5*S*)-4-Acetamido-5-((4-(methyl(phenyl)amino)benzyl)amino)-3-(pent**
15 **an-3-yloxy)cyclohex-1-ene-1-carboxylic acid (26b)**. White powder, 63% yield, mp:
16 209.8-211.2°C. ¹H NMR (400 MHz, DMSO-*d*₆): δ 8.10 (d, *J* = 8.9 Hz, 1H, NH),
17 7.43-7.27 (m, 4H, Ph-H), 7.11-6.98 (m, 3H, Ph-H), 6.94 (d, *J* = 8.5 Hz, 2H, Ph-H),
18 6.64 (s, 1H, CH), 4.21 (d, *J* = 7.3 Hz, 1H, CH), 4.03 (overlapped, 3H, CH₂, CH),
19 3.33-3.22 (overlapped, 4H, CH₃, CH), 2.92-2.80 (m, 1H, CH), 2.59 (d, *J* = 11.0 Hz,
20 1H, CH), 1.91 (s, 3H, CH₃), 1.52-1.33 (m, 4H, 2CH₂), 0.82 (dt, *J* = 18.2, 7.3 Hz, 6H,
21 2CH₃). ¹³C NMR (100 MHz, DMSO-*d*₆): δ 170.1, 166.2, 149.2, 147.7, 138.4, 129.5,
22 129.3, 129.0, 121.1, 120.9, 119.6, 81.3, 75.6, 60.8, 54.8, 54.3, 49.6, 26.0, 25.6, 23.5,
23 14.5, 9.9, 9.4. HRMS calcd for C₂₈H₃₇N₃O₄ [M + H]⁺: 480.2857. Found: m/z
24 480.2853. HPLC purity: 95.94% (295 nm).
25
26
27
28
29
30
31
32
33
34
35
36

37 **(3*R*,4*R*,5*S*)-4-Acetamido-5-((4-(ethyl(phenyl)amino)benzyl)amino)-3-(pentan**
38 **-3-yloxy)cyclohex-1-ene-1-carboxylic acid (26c)**. White powder, 65% yield, mp:
39 158.5-160.2°C. ¹H NMR (400 MHz, DMSO-*d*₆): δ 7.94 (d, *J* = 9.1 Hz, 1H, NH), 7.22
40 (dt, *J* = 8.6, 3.6 Hz, 4H, Ph-H), 6.97-6.88 (m, 3H, Ph-H), 6.79 (d, *J* = 8.7 Hz, 2H,
41 Ph-H), 6.54 (s, 1H, CH), 4.08 (d, *J* = 8.1 Hz, 1H, CH), 3.99-3.79 (m, 3H), 3.65 (q, *J* =
42 7.0 Hz, 2H, CH₂), 3.18-3.09 (m, 1H, CH), 2.73 (dd, *J* = 17.2, 4.9 Hz, 1H, CH),
43 2.51-2.41 (m, 1H, CH), 2.20-1.60 (overlapped, 4H, CH, CH₃), 1.33 (ddq, *J* = 19.1,
44 13.1, 6.9 Hz, 4H, 2CH₂), 1.02 (t, *J* = 7.0 Hz, 3H, CH₃), 0.71 (dt, *J* = 17.4, 7.4 Hz, 6H,
45 2CH₃). ¹³C NMR (100 MHz, DMSO-*d*₆): δ 171.0, 167.4, 147.9, 147.2, 137.8, 131.2,
46 129.3, 129.0, 121.1, 120.9, 119.6, 81.3, 75.6, 60.8, 54.8, 54.3, 49.6, 26.0, 25.6, 23.5,
47 14.5, 9.9, 9.4. HRMS calcd for C₂₉H₃₉N₃O₄ [M + H]⁺: 494.2909. Found: m/z
48 494.2905. HPLC purity: 95.94% (295 nm).
49
50
51
52
53
54
55
56
57
58
59
60

1
2
3 129.9, 128.4, 122.9, 118.9, 81.5, 75.1, 54.4, 51.7, 46.7, 46.2, 30.8, 26.0, 25.5, 23.8,
4
5 12.8, 9.8, 9.3. HRMS calcd for C₂₉H₃₉N₃O₄ [M + H]⁺: 494.3013. Found: m/z
6
7 494.3090. HPLC purity: 96.02% (298 nm).
8

9 **Synthesis of Compound 28.** The synthetic method was similar to that of
10
11 **14a-14d**, starting from **27**.
12

13 **Ethyl(3*R*,4*R*,5*S*)-5-((4-(1*H*-pyrrol-1-yl)benzyl)amino)-4-acetamido-3-(penta**
14 **-3-yloxy)cyclohex-1-ene-1-carboxylate (28a).** White powder, 64% yield, mp:
15
16 144.1-145.1°C. ¹H NMR (400 MHz, DMSO-*d*₆): δ 7.72 (d, *J* = 9.0 Hz, 1H, NH), 7.41
17
18 (d, *J* = 8.4 Hz, 2H, Ph-H), 7.28 (d, *J* = 8.4 Hz, 2H, Ph-H), 7.23 (t, *J* = 2.2 Hz, 2H,
19
20 pyrrole-H), 6.54 (s, 1H, CH), 6.17-6.10 (m, 2H, pyrrole-H), 4.04 (q, *J* = 7.0 Hz, 2H,
21
22 CH₂), 3.92 (d, *J* = 7.8 Hz, 1H, NH), 3.72 (t, *J* = 12.3 Hz, 1H, CH), 3.64 (t, *J* = 9.2 Hz,
23
24 2H, CH₂), 3.23-3.17 (m, 1H, CH), 2.77-2.63 (m, 1H, CH), 2.58 (dd, *J* = 17.5, 4.5 Hz,
25
26 1H, CH), 2.04 (dd, *J* = 15.4, 9.1 Hz, 1H, CH), 1.76 (s, 3H, CH₃), 1.32 (qt, *J* = 14.2,
27
28 7.2 Hz, 4H, 2CH₂), 1.11 (t, *J* = 7.1 Hz, 3H, CH₃), 0.71 (dt, *J* = 14.4, 7.4 Hz, 6H,
29
30 2CH₃). ¹³C NMR (100 MHz, DMSO-*d*₆): δ 170.1, 166.2, 139.1, 138.4, 129.7, 128.9,
31
32 119.5, 119.3, 110.7, 81.3, 75.6, 60.8, 54.8, 54.2, 49.2, 30.4, 26.0, 25.6, 23.5, 14.5, 9.9,
33
34 9.4. ESI-MS: m/z 468.4 [M + H]⁺, C₂₇H₃₇N₃O₄ (467.61).
35
36
37
38
39

40 **Ethyl(3*R*,4*R*,5*S*)-5-((4-(1*H*-pyrazol-1-yl)benzyl)amino)-4-acetamido-3-(penta**
41 **n-3-yloxy)cyclohex-1-ene-1-carboxylate (28b).** Pale yellow sticky oil, 58% yield. ¹H
42
43 NMR (400 MHz, DMSO-*d*₆): δ 8.37 (d, *J* = 2.5 Hz, 1H, NH), 7.77 (d, *J* = 9.0 Hz, 1H,
44
45 pyrazole-H), 7.71 (d, *J* = 8.1 Hz, 2H, Ph-H), 7.62 (d, *J* = 1.7 Hz, 1H, pyrazole-H),
46
47 7.36 (d, *J* = 8.1 Hz, 2H, Ph-H), 6.54 (s, 1H, CH), 6.42 (t, *J* = 2.1 Hz, 1H, pyrazole-H),
48
49 4.04 (q, *J* = 7.0 Hz, 2H, CH₂), 3.96 (d, *J* = 7.4 Hz, 1H, NH), 3.86 (d, *J* = 11.9 Hz, 1H,
50
51 CH), 3.73 (dt, *J* = 17.6, 10.1 Hz, 2H, 2CH), 3.40-3.10 (m, 2H, 2CH), 2.94-2.73 (m,
52
53 1H, CH), 2.68-2.53 (m, 1H, CH), 2.26-2.01 (m, 1H, CH), 1.77 (s, 3H, CH₃), 1.29 (qt,
54
55
56
57
58
59
60

1
2
3 $J = 13.9, 5.5$ Hz, 4H, 2CH₂), 1.11 (t, $J = 7.1$ Hz, 3H, CH₃), 0.70 (dt, $J = 14.6, 7.4$ Hz,
4
5 6H, 2CH₃). ¹³C NMR (100 MHz, DMSO-*d*₆): δ 170.5, 166.0, 141.3, 139.4, 138.4,
6
7 131.9, 130.1, 129.1, 128.5, 128.0, 118.6, 108.2, 81.4, 75.3, 60.9, 54.7, 53.5, 48.5, 26.0,
8
9 25.6, 23.6, 23.2, 14.5, 9.8, 9.4. ESI-MS: m/z 469.4 [M + H]⁺, C₂₆H₃₆N₄O₄ (468.60).

11
12 **Synthesis of Compound 29.** The synthetic method was similar to that of
13
14 **15a-15d**, starting from **28**.

15
16 **(3*R*,4*R*,5*S*)-5-((4-(1*H*-Pyrrol-1-yl)benzyl)amino)-4-acetamido-3-(pentan-3-yl**
17
18 **oxy)cyclohex-1-ene-1-carboxylic acid (29a).** White powder, 66% yield, mp:
19
20 119.5-124.9°C. ¹H NMR (400 MHz, DMSO-*d*₆): δ 8.08 (d, $J = 8.9$ Hz, 1H, NH), 7.62
21
22 (d, $J = 8.5$ Hz, 2H, Ph-H), 7.55 (d, $J = 8.3$ Hz, 2H, Ph-H), 7.43-7.36 (m, 2H,
23
24 pyrrole-H), 6.64 (s, 1H, CH), 6.32-6.22 (m, 2H, pyrrole-H), 4.19 (d, $J = 7.4$ Hz, 1H,
25
26 NH), 4.08 (q, $J = 12.8$ Hz, 2H, 2CH), 3.94 (q, $J = 9.1$ Hz, 2H, CH₂), 3.32-3.05 (m,
27
28 2CH), 2.91-2.79 (m, 1H, CH), 2.60-2.40 (m, 1H, CH), 1.92 (s, 3H, CH₃), 1.55-1.33 (m,
29
30 4H, 2CH₂), 0.89-0.75 (m, 6H, 2CH₃). ¹³C NMR (100 MHz, DMSO-*d*₆): δ 170.9,
31
32 167.5, 140.1, 137.9, 131.3, 128.6, 119.3, 111.0, 81.5, 75.2, 54.4, 52.0, 46.6, 27.4, 26.0,
33
34 25.5, 23.8, 9.8, 9.3. HRMS calcd for C₂₅H₃₃N₃O₄ [M + H]⁺: 440.2544. Found: m/z
35
36 440.2539. HPLC purity: 96.94% (259 nm).

37
38
39 **(3*R*,4*R*,5*S*)-5-((4-(1*H*-Pyrazol-1-yl)benzyl)amino)-4-acetamido-3-(pentan-3-y**
40
41 **loxy)cyclohex-1-ene-1-carboxylic acid (29b).** White powder, 61% yield, mp:
42
43 113.1-115.2°C. ¹H NMR (400 MHz, DMSO-*d*₆): δ 8.55 (d, $J = 2.4$ Hz, 1H, NH), 8.14
44
45 (d, $J = 9.0$ Hz, 1H, pyrazole-H), 7.89 (d, $J = 8.5$ Hz, 2H, Ph-H), 7.76 (d, $J = 1.4$ Hz,
46
47 1H, pyrazole-H), 7.65 (d, $J = 8.4$ Hz, 2H, Ph-H), 6.65 (s, 1H, CH), 6.58-6.54 (m, 1H,
48
49 pyrazole-H), 4.33-4.08 (m, 3H, CH₂, CH), 3.99 (q, $J = 8.6$ Hz, 1H, CH), 3.60-3.20
50
51 (overlapped, 2H, 2CH), 2.90 (dd, $J = 17.0, 4.3$ Hz, 1H, CH), 2.70-2.54 (m, 1H, CH),
52
53 1.93 (s, 3H, CH₃), 1.53-1.33 (m, 4H, 2CH₂), 0.82 (dt, $J = 16.9, 7.4$ Hz, 6H, 2CH₃). ¹³C
54
55

1
2
3 NMR (100 MHz, DMSO-*d*₆): δ 171.1, 167.3, 141.6, 140.1, 138.0, 131.6, 130.8, 128.3,
4
5 128.2, 118.6, 108.5, 81.5, 75.0, 54.3, 51.5, 46.0, 26.7, 26.0, 25.5, 23.9, 9.8, 9.3.
6
7 HRMS calcd for C₂₄H₃₂N₄O₄ [M + H]⁺: 441.2496. Found: m/z 441.2498. HPLC
8
9 purity: 98.45% (257 nm).

11 **Synthesis of Lead Compound 6 (No. 32, J. Med. Chem. 2014, 57, 8445-8458).**

12
13 Lead compound **6** was synthesized according to the literature procedure.³³

14
15
16 **4-(Thiophen-2-yl)benzaldehyde (30)**. Pale yellow crystal powder, 68% yield,
17
18 mp: 64.2-66.1°C. ¹H NMR (400 MHz, DMSO-*d*₆): δ 10.01 (s, 1H, CH), 7.96-7.92 (m,
19
20 2H, Ph-H), 7.92-7.88 (m, 2H, Ph-H), 7.74 (dd, *J* = 3.7, 1.1 Hz, 1H, thiophene-H),
21
22 7.71 (dd, *J* = 5.1, 1.1 Hz, 1H, thiophene-H), 7.22 (dd, *J* = 5.1, 3.7 Hz, 1H,
23
24 thiophene-H). ¹³C NMR (100 MHz, DMSO-*d*₆): δ 192.7, 142.3, 139.7, 135.3, 130.8,
25
26 129.4, 128.4, 126.44, 126.1. ESI-MS: m/z 189.3 [M + H]⁺: C₁₁H₈OS (188.24).

27
28
29 **Ethyl(3*R*,4*R*,5*S*)-4-acetamido-3-(pentan-3-yloxy)-5-((4-(thiophen-2-yl)benzyl**
30
31 **)amino)cyclohex-1-ene-1-carboxylate (31)**. White powder, 68% yield, mp: 139.2-
32
33 144.1°C. ¹H NMR (400 MHz, DMSO-*d*₆): δ 7.82 (d, *J* = 9.1 Hz, 1H, NH), 7.60 (d, *J* =
34
35 8.2 Hz, 2H, Ph-H), 7.52 (dd, *J* = 5.1, 1.0 Hz, 1H, thiophene-H), 7.48 (dd, *J* = 3.6, 1.0
36
37 Hz, 1H, thiophene-H), 7.35 (d, *J* = 8.2 Hz, 2H, Ph-H), 7.13 (dd, *J* = 5.0, 3.6 Hz, 1H,
38
39 thiophene-H), 6.64 (s, 1H, NH), 4.14 (q, *J* = 7.0 Hz, 2H, CH₂), 4.01 (d, *J* = 8.0 Hz, 1H,
40
41 NH), 3.85-3.64 (m, 3H, CH₂, CH), 3.40-3.35 (m, 1H, CH), 2.75 (dt, *J* = 14.9, 7.4 Hz,
42
43 1H, CH), 2.67 (dd, *J* = 17.5, 4.8 Hz, 1H, CH), 2.24-1.90 (m, 2H, 2CH), 1.87 (s, 3H,
44
45 CH₃), 1.50-1.34 (m, 4H, 2CH₂), 1.22 (t, *J* = 7.1 Hz, 3H, CH₃), 0.82 (dt, *J* = 14.4, 7.4
46
47 Hz, 6H, 2CH₃). ¹³C NMR (100 MHz, DMSO-*d*₆): δ 170.0, 166.2, 140.9, 132.5, 129.0,
48
49 128.9, 125.7, 125.6, 123.7, 81.3, 75.7, 60.8, 54.8, 54.5, 49.7, 30.8, 26.0, 25.6, 23.5,
50
51 14.5, 9.9, 9.4. ESI-MS: m/z 485.5[M + H]⁺, C₂₇H₃₆N₂O₄S (484.66).

52
53
54
55 **(3*R*,4*R*,5*S*)-4-Acetamido-3-(pentan-3-yloxy)-5-((4-(thiophen-2-yl)benzyl)ami**

no)cyclohex-1-ene-1-carboxylic acid (6). White powder, 74% yield, mp: 170.1-172.5°C. ¹H NMR (400 MHz, CD₃OD): δ 7.73 (d, *J* = 8.1 Hz, 2H, Ph-H), 7.51 (d, *J* = 8.1 Hz, 2H, Ph-H), 7.45 (d, *J* = 3.4 Hz, 1H, thiophene-H), 7.42 (d, *J* = 4.9 Hz, 1H, thiophene-H), 7.14-7.07 (m, 1H, thiophene-H), 6.87 (s, 1H, CH), 4.41 (d, *J* = 13.1 Hz, 1H, CH), 4.27 (d, *J* = 13.3 Hz, 2H, CH₂), 4.23-4.16 (m, 1H, CH), 3.64 (td, *J* = 10.2, 5.6 Hz, 1H, CH), 3.45 (p, *J* = 5.5 Hz, 1H, CH), 3.06 (dd, *J* = 17.3, 5.2 Hz, 1H, CH), 2.67 (dd, *J* = 17.2, 10.0 Hz, 1H, CH), 2.06 (s, 3H, CH₃), 1.60-1.46 (m, *J* = 6.6 Hz, 4H, 2CH₂), 0.90 (q, *J* = 7.6 Hz, 6H, 2CH₃). ¹³C NMR (100 MHz, CD₃OD): δ 173.5, 167.1, 142.7, 137.3, 135.7, 130.3, 129.6, 127.9, 127.2, 125.9, 125.3, 123.7, 82.3, 74.5, 54.9, 51.5, 47.1, 25.8, 25.7, 25.2, 22.0, 8.4, 8.1. HRMS calcd for C₂₅H₃₂N₂O₄S [M + H]⁺: 457.2156, Found: *m/z* 457.2154. HPLC purity: 99.77% (289 nm).

Influenza Virus NA-Inhibitory Assay

The NA inhibition assay was conducted according to the standard method.⁵² The NAs (A/Anhui/1/2005 (H5N1-H274Y mutation), A/PuertoRico/8/1934 (H1N1), A/Babol/36/2005 (H3N2), A/Anhui/1/2013 (H7N9) and A/California/04/2009 (09N1)) were obtained from Sino Biological Inc. and diluted suspensions of influenza viruses (H5N1, H5N2, H5N6, H5N8, H9N2) were harvested from the allantoic fluid of influenza virus-infected embryonated chicken eggs. All of them were used for biological evaluation. The fluorogenic substrate, 2'-(4-methylumbelliferyl)- α -D-acetylneuraminic acid sodium salt hydrate (4-MU-NANA) (Sigma, M8639), was cleaved by NA to afford a quantifiable fluorescent product. Test compounds were dissolved in DMSO first, and then diluted to the required concentrations in MES buffer (3.54 g 2-(N-morpholino)ethanesulfonic acid and 0.185 g CaCl₂ in 400 mL Milli-Q water). To a 96-well fluorescent plate, 10 μ L of the diluted virus supernatant or NA assay diluent, 70 μ L of MES buffer, and 10 μ L of compounds at different concentrations were added

1
2
3 successively, and the plate was incubated for 10 min at 37°C. The reaction was started
4
5 by the addition 10 μ L of fluorogenic substrate. After incubation for 40-60 min, the
6
7 reaction was terminated by adding 150 μ L of termination solution (6.01 g glycine and
8
9 3.20 g NaOH in 400 mL Milli-Q water). Fluorescence was measured with microplate
10
11 reader (Thermo Scientific Microplate Reader) (excitation at 355 nm, emission at 460
12
13 nm). Substrate blanks were subtracted from the sample readings. The 50%-inhibitory
14
15 concentration (IC_{50}) values were determined from the dose-response curves by
16
17 plotting the percent inhibition of NA activity versus inhibitor concentrations.
18
19

20 **Cells and Viruses**

21
22 Chicken embryo fibroblasts (CEFs) were maintained in Dulbecco's modified Eagle's
23
24 medium (DMEM, Thermo Fisher Scientific) supplemented with 5% (vol/vol) fetal
25
26 bovine serum (FBS, Thermo Fisher Scientific). The cells were maintained at 37°C in a
27
28 humidified atmosphere supplemented with 5% CO₂. Madin-Darby Canine Kidney
29
30 (MDCK) cells were maintained in Dulbecco's modified Eagle's medium (DMEM,
31
32 Life Biotechnologies) supplemented with 10% (vol/vol) fetal bovine serum (FBS, Life
33
34 Biotechnologies) and antibiotics (100 U/mL penicillin and 100 μ g/mL streptomycin,
35
36 Life Technologies). The cells were maintained at 37°C in a humidified atmosphere
37
38 supplemented with 5% CO₂.
39
40

41
42 Influenza H5N1, H5N2, H5N6, and H5N8 virus was obtained from Institute of
43
44 Poultry Science, Shandong Academy of Agricultural Sciences. Influenza A/PR/8/34
45
46 virus (PR8) (H1N1, Cambridge lineage) was obtained from P. Digard (Roslin Institute,
47
48 University of Edinburgh, United Kingdom). The H3N2 virus A/Wisconsin/67/05
49
50 (WSN) was provided by R. Cusinato (Clinical Microbiology and Virology Unit,
51
52 Padua University Hospital, Padua, Italy).
53

54 **Determination of EC_{50} and CC_{50} of NA Inhibitors in CEFs**

1
2
3 The anti-flu activity and cytotoxicity of the newly synthesized compounds were
4
5 evaluated as described by Shie et al.⁵³ with minor modifications. Results were
6
7 expressed as EC₅₀ values, which are the concentrations affording 50% protection
8
9 against H5N1, H5N2, H5N6, and H5N8 virus infection-mediated cytopathic effects
10
11 (CPE). Aliquots of 50 μL of diluted H5N1, H5N2, H5N6, H5N8 at 50 TCID₅₀ were
12
13 mixed with equal volumes of solutions of the newly synthesized compounds in serial
14
15 two-fold dilutions in assay media (1% FBS in DMEM). The mixtures were used to
16
17 infect 100 μL of CEFs at 1×10^5 cells/mL in 96-well plates. The plates were incubated
18
19 for 48 h at 37°C under 5.0% CO₂ in air, then 100 μL per well of Cell Counting Kit-8
20
21 (CCK-8, Dojindo Laboratories) reagent solution (10 μL CCK-8 and 90 μL media) was
22
23 added. After incubation at 37°C for 90 min, the absorbance at 450 nm was read on a
24
25 microplate reader. Inhibitor EC₅₀ values were determined by fitting the curve of
26
27 percent cytopathic effect (CPE) versus NA inhibitor concentration. OSC and
28
29 zanamivir were used as reference compounds at the same time. The CC₅₀ value was
30
31 employed as a measure of the cytotoxicity of newly synthesized compounds to CEF
32
33 and was determined in the same manner as EC₅₀, but without virus infection.
34
35
36

37 **Plaque Reduction Assay (PRA) in MDCK Cells**

38
39 The antiviral activity of selected compounds against the influenza A PR8 and
40
41 WSN viruses was tested by PRA as previously described,^{54,55} with some modifications.
42
43 For plaque reduction assays (PRA), MDCK cells were seeded at a density of 7×10^5
44
45 cells per well in 12-well plates. The next day, the culture medium was removed and
46
47 the monolayers were first washed with serum-free DMEM, and then infected with
48
49 FluA virus (PR8 or WSN strain) at 30-40 PFU/well in DMEM supplemented with
50
51 0.14% BSA and 2 μg/mL TPCK-treated trypsin (Worthington Biochemical
52
53 Corporation) for 1 h at 37°C. Cells were then incubated with medium containing 1.2%
54
55
56
57
58
59
60

(wt/vol) Avicel cellulose, 0.14% BSA, 2 $\mu\text{g}/\text{mL}$ TPCK-treated trypsin, and different concentrations of each test compound. After 2 days of incubation, cell monolayers were fixed with 4% (vol/vol) formaldehyde and stained with 0.1% toluidine blue, and viral plaques were counted. Oseltamivir and Zanamivir were included in each experiment as reference compounds. Values obtained from the wells treated with only DMSO were set as 100% of plaque formation.

Citotoxicity Assay in MDCK Cells

Cytotoxicity of selected compounds was assessed in MDCK cells by the 3-(4,5-dimethylthiazol-2-yl)-2,5-diphenyltetrazolium bromide (MTT) method, as previously described.^{56,57} MDCK cells (seeded at a density of 2×10^4 cells per well) were grown in 96-well plates for 24 hours and then treated with serial dilutions of test compounds, or DMSO as a control, in DMEM supplemented with 10% FBS. After incubation at 37°C for 48 hours, 5 mg/ml of MTT (Sigma) in PBS was added into each well and incubated at 37°C for further 4 hours. Successively, a solubilizing solution (10% SDS, 0.01 N HCl) was added to dissolve the formazan salt and lyse the cells, and incubated O/N at 37°C. Finally, absorbance was read at the wavelength of 620 nm using an ELISA microplate reader (Tecan Sunrise). Values obtained from the wells treated with only DMSO were set as 100% of viable cells.

Computational Modeling

Preparation of Ligand and Protein Structures

The 3D conformations of OSC and compound **15b** were built using the Maestro module.⁵⁸ Subsequently, the ligands were preprocessed using the LigPrep module of the Schrödinger Suite⁵⁹ (determination of protonation states using the Epik tool and energy minimization). The ligands were minimized using the MMFF95S force field.

1
2
3 The atomic coordinates of six subtypes of neuraminidases were extracted from
4 the Protein Data Bank (N1: 2HU0³⁰, resolution: 2.95 Å; N2: 4K1I³¹, resolution: 1.8 Å;
5 N6: 5HUM⁶⁰, resolution: 1.6 Å; N8: 2HT7³⁰, resolution: 2.6 Å, N9: 5L15⁶¹, resolution:
6 2.4 Å and 09N1: 3NSS³², resolution: 1.90 Å). Two forms of X-ray crystal structures
7 have been deposited for NA, one being an “open form” in which the 150-cavity is
8 accessible from the main ligand binding pocket and other being the closed form in
9 which the 150-cavity is inaccessible. Subtypes N1 and N8 are in open forms and the
10 remaining four subtypes (N2, N6, N9, and 09N1) are in closed form. In order to
11 understand the binding mode of compound **15b** in all six subtypes, open forms of the
12 N2, N6, N9 and 09N1 structures were modeled at the loop region (residues between
13 Gly147-Ser153) based on the N1 structure as the template. The modeled region was
14 subsequently relaxed by energy minimization. Each protein structure further
15 optimized with the Protein Preparation Wizard⁶² using the Schrödinger Suite. This
16 optimization includes adding hydrogen atoms, assigning bond orders, and building
17 disulfide bonds. The protonation states of the ionizable residues (at pH 7.0) were
18 predicted by the PROPKA tool⁶³ provided in the Protein Preparation Wizard. An
19 optimized structure model was finally found by energy minimization (i.e., only
20 positions of the hydrogen atoms) using the OPLS2005 force field.
21
22
23
24
25
26
27
28
29
30
31
32
33
34
35
36
37
38
39
40
41

42 ***Generation of Ligand Binding Conformation***

43
44

45 The initial binding conformation of a ligand in the protein was generated based
46 on the docking methodology. The receptor grid generation module of Glide⁶⁴ was
47 used to define the active site for the docking. As the N1 and N8 crystal structures have
48 a bound ligand (OSC), the centroid of the grid box (of size 20 Å) was placed at this
49 ligand, while for rest of the structures (N2, N6, N9, 09N1), key residues in the active
50 site (which covers both the 150-cavity and ligand pocket) were set as the center of the
51
52
53
54
55
56
57
58
59
60

1
2
3 grid box (of size 20 Å). Water molecules at the active site located more than 3 Å from
4 the bound ligand were deleted. The docking and scoring function (Standard precision)
5 parameters and settings were chosen as defaults in this study. A proper starting
6 configuration of a given ligand-protein complex represents a crucial step for
7 molecular dynamics simulation studies. Therefore, both OSC and **15b** ligands were
8 docked, and the top-ranked 10 ligand poses were saved for further binding pose
9 analysis and used for MD simulation studies. In total, 12 protein-ligand complexes (2
10 ligands × 6 NA structures) were chosen based on the protein-ligand interactions for
11 explicit solvent MD simulations study.
12
13
14
15
16
17
18
19
20
21

22 ***Molecular Dynamics Simulations***

23
24
25 Before conducting the MD simulations, we optimized OSC and **15b** geometry at
26 the level of B3LYP/6-31G(d) using Gaussian 09⁶⁵ and the atomic charges were
27 calculated from the electrostatic potential (ESP) using density functional theory at the
28 level of B3LYP/6-31G(d) with the PCM solvation model. These atomic charges were
29 obtained using the CHELPG procedure⁶⁶ as implemented in Gaussian 09.
30
31
32
33
34
35

36 All MD simulations were performed and analyzed using the Amber 14
37 software.⁶⁷ The General Amber Force Field (GAFF) was used to describe the
38 dispersion interaction of ligands with enzymes and solvents. The Amber FF99SB
39 force field was used to describe the protein interactions. Subsequently, TIP3P water
40 (solvent) molecules were added with a 12 Å buffering distance from the protein edge
41 atoms and an orthorhombic simulation box was chosen. Suitable counter ions were
42 also added to neutralize the system (4 Na⁺ ions for N1, 3 Na⁺ ions for N2 and ON91, 2
43 Na⁺ ions for N6 and N8). The *tleap* tool in the Amber suite was used to build
44 coordinate and topology files. The disulphide bonds were built using the crystal
45 structure information between pairs of residues for N2 subtype namely, 11-336, 43-48,
46
47
48
49
50
51
52
53
54
55
56
57
58
59
60

1
2
3 94-112, 102-149, 151-156, 197-210, 199-208, 237-256, and 340-366. Energy
4
5 minimization was carried out in two steps; first, the system (ligand and solvents) was
6
7 minimized using the steepest descent minimization with all heavy atoms restrained.
8
9 The maximum number of minimization steps was set to 5000. In the second stage of
10
11 the minimization, the entire system was energy-minimized. To avoid edge effects,
12
13 periodic boundary conditions were applied during the MD simulations. In the process
14
15 of thermalization, initial velocities were generated from a Maxwell-Boltzmann
16
17 distribution at 100 K, and the system temperature was gradually increased to 300 K at
18
19 constant volume over a 500 ps MD simulation. After the thermalization process, the
20
21 system was equilibrated at constant temperature (300 K) and pressure (1 bar) using
22
23 the Berendsen coupling algorithm⁶⁸ for another 2 ns MD simulation. After the
24
25 equilibration step, the MD production run was started for 20 ns using a time step of 2
26
27 fs. Coordinates were saved every 2 ps from the last 5 ns simulation for analysis (in
28
29 total, 500 snapshots).
30
31

32 33 **Acute Toxicity Experiment**⁶⁹

34 35 **Animals**

36
37 Kunming mice (20-30 g and 4-5 weeks old) were purchased from the animal
38
39 experimental center of Shandong University. All animal treatments were performed
40
41 strictly in accordance with the institutional guidelines of Animal Care and Use
42
43 Committee at Shandong University, after gaining approved by the Animal Ethical and
44
45 Welfare Committee (AEWC). We performed this study with an authorized standard
46
47 method to detect acute toxicity using mice and accredited by Laboratory Animal
48
49 Ethical and Welfare Committee of Shandong University Cheeloo College of Medicine.
50
51 Animals were housed at $22 \pm 2^\circ\text{C}$ and relative humidity was $50 \pm 10\%$. A 12 h light
52
53 and 12 h dark cycle was maintained. Animals were given free access to food and
54
55
56
57
58
59
60

1
2
3 water.

4 5 **Materials and Methods**

6
7 To investigate the acute toxicity of compound **15b** in mice, we used 30 healthy
8 Kunming mice (5 males and 5 females per group) and divided them into three groups
9 of five mice each. **15b** was suspended in PEG-400 and water (V:V = 1:3) at
10 concentrations of 0.05 and 0.1 g·mL⁻¹, respectively, and administered intragastrically
11 by gavage after the mice had been fasted overnight (12 h). Dosages of 0.5 and 1 g·kg⁻¹
12 were administered to two groups of mice (5 males and 5 females per group). Blank
13 control (without **15b**) was employed at the same time. Death, body weight and
14 behavior (death, lethargy, clonic convulsion, anorexia, ruffled fur and no abnormality)
15 were monitored every day. At the end of the experiment, all animals were sacrificed
16 for subsequent experimental studies.
17
18
19
20
21
22
23
24
25
26
27
28
29
30

31 **ASSOCIATED CONTENT**

32 33 34 35 **Supporting Information**

36 The Supporting Information is available free of charge via the Internet at
37 <http://pubs.acs.org>.
38

39
40
41
42 Phylogenetic tree, influenza virus B NA inhibitory activities of oseltamivir
43 derivatives, MD simulation figures, amino acid sequences of the NAs
44 (A/goose/Guangdong/SH7/2013 (H5N1), A/Chicken/Hebei/LZF/2014 (H5N2),
45 A/duck/Guangdong/674/2014 (H5N6), A/goose/Jiangsu/1306/2014 (H5N8)
46 A/chicken/china/415/2013 (H9N2) and A/Anhui/1/2013 (H7N9)), determination
47 of influenza virus TCID₅₀, TCID₅₀ of H5N1, H5N2, H5N6, and H5N8 in CEFs
48 and MDCK cells, stability in human plasma and metabolic stability in human
49
50
51
52
53
54
55
56

1
2
3 liver microsomes, figures of body weight of acute toxicity experiment and in vivo
4
5 pharmacokinetics study.

6
7 Molecular formula strings.
8
9

10 11 **AUTHOR INFORMATION**

12 13 **Corresponding Authors**

14
15 *B.H.: e-mail, hbind@163.com; phone, 086-531-85999436;

16
17 *P.Z.: e-mail, zhanpeng1982@sdu.edu.cn; phone, 086-531-88382005;

18
19 *X.L.: e-mail, xinyongl@sdu.edu.cn; phone, 086-531-88380270.
20
21

22 23 **Notes**

24 The authors declare that all experimental work complied with the institutional
25
26 guidelines on animal studies (care and use of laboratory animals).
27

28 The authors declare no competing financial interest.
29
30
31
32

33 34 **ACKNOWLEDGMENTS**

35 Financial support from the National Natural Science Foundation of China (NSFC no.
36
37 81773574), Shandong Provincial Key Research and Development Program (no.
38
39 2015GNC110009), the Science and Technology Development Project of Shandong
40
41 Province (no. 2014GSF118175), Young Scholars Program of Shandong University
42
43 (YSPSDU No. 2016WLJH32), Major Project of Science and Technology of Shandong
44
45 Province (no. 2015ZDJS04001), Key research and development project of Shandong
46
47 Province (no. 2017CXGC1401), from the University of Padua, Progetto di Ricerca di
48
49 Ateneo 2014 grant n. CPDA141311(to Arianna Loregian), and from Associazione
50
51 Italiana per la Ricerca sul Cancro (AIRC), Investigator Grant n. 18855 (to Arianna
52
53 Loregian). We are very grateful to Dr. Xiuli Ma and Min Shang at Shandong Academy
54
55
56
57
58
59
60

1
2
3 of Agricultural Sciences for their work in the biological activity assays.
4
5

6
7 **ABBREVIATIONS USED**
8

9 AIV, Avian influenza virus; CEF, chicken embryo fibroblasts; DMSO, dimethyl
10 sulphoxide; CCK8, cell counting kit-8; CC₅₀, 50% cytotoxicity concentration; DMEM,
11 Dulbecco's modified Eagle's medium, CPE, cytopathic effects; EC₅₀, the
12 concentration causing 50% inhibition of antiviral activity; FBS, fetal bovine serum,
13 HA, hemagglutinin; MD, molecular dynamics, MDCK, Madin-Darby Canine Kidney
14 cells, HLM, human liver microsome; MUNANA, 2'-(4-methyl-
15 umbelliferyl)- α -D-N-acetylneuraminic acid; NA, neuraminidase; 09N1, NA of
16 H1N1pdm09; NAIs neuraminidases inhibitors; OSC, oseltamivir carboxylate; PRA,
17 plaque reduction assay, SAR, structure-activity relationship; TMS, tetramethylsilane;
18 TLC, thin-layer chromatography; TCID₅₀, 50% tissue culture infectious dose; PR8,
19 A/PR/8/34 virus, WSN, A/Wisconsin/67/05.
20
21
22
23
24
25
26
27
28
29
30
31
32
33
34
35
36
37
38
39
40
41
42
43
44
45
46
47
48
49
50
51
52
53
54
55
56
57
58
59
60

REFERENCES

- (1) Wang, M.; Qi, J.; Liu, Y.; Vavricka, C. J.; Wu, Y.; Li, Q.; Gao, G. F. Influenza A virus N5 neuraminidase has an extended 150-cavity. *J. Virol.* **2011**, *85*, 8431–8435.
- (2) Lin, C. H.; Chang, T. C.; Das, A.; Fang, M. Y.; Hung, H. C.; Hsu, K. C.; Yang, J. M.; von Itzstein, M.; Mong, K. K.; Hsu, T. A.; Lin, C. C. Synthesis of acylguanidine zanamivir derivatives as neuraminidase inhibitors and the evaluation of their bio-activities. *Org. Biomol. Chem.* **2013**, *11*, 3943–3948.
- (3) Grienke, U.; Schmidtke, M.; Kirchmair, J.; Pfarr, K.; Wutzler, P.; Dürrwald, R.; Wolber, G.; Liedl, K. R.; Stuppner, H.; Rollinger, J. M. Antiviral potential and molecular insight into neuraminidase inhibiting diaryl heptanoids from alpinia katsumadai. *J. Med. Chem.* **2010**, *53*, 778–786.
- (4) World Health Organization Influenza Fact Sheet 211; World Health Organization: Geneva, **2018**; <http://www.who.int/mediacentre/factsheets/fs211/en/> (accessed January 31, 2018).
- (5) Cox, N. J. and Subbarao, K. Global epidemiology of influenza: past and present. *Annu. Rev. Med.* **2000**, *51*, 407–421.
- (6) Moorthy, N. S.; Poongavanam, V.; Pratheepa, V. Viral M2 ion channel protein: a promising target for anti-influenza drug discovery. *Mini. Rev. Med. Chem.* **2014**, *14*, 819–830.
- (7) Novel Swine-Origin Influenza A (H1N1) Virus Investigation Team; Dawood, F. S.; Jain, S.; Finelli, L.; Shaw, M. W.; Lindstrom, S.; Garten, R. J.; Gubareva, L. V.; Xu, X.; Bridges, C. B.; Uyeki, T. M. Emergence of a novel swine-origin influenza A (H1N1) virus in humans. *N. Engl. J. Med.* **2009**, *360*, 2605–2615.
- (8) Sartore, S.; Bonfanti, L.; Lorenzetto, M.; Cecchinato, M.; Marangon, S. The effects of control measures on the economic burden associated with epidemics of

- 1
2
3 avian influenza in Italy. *Poult. Sci.* **2010**, *89*, 1115-1121.
- 4
5 (9) Alexander, D. J. Should we change the definition of avian influenza for eradication
6
7 purposes?. *Avian Dis.* **2003**, *47*, 976–981.
- 8
9 (10) Xu, H.; Meng, F.; Huang, D.; Sheng, X.; Wang, Y.; Zhang, W.; Chang, W.; Wang,
10
11 L.; Qin, Z. Genomic and phylogenetic characterization of novel, recombinant H5N2
12
13 avian influenza virus strains isolated from vaccinated chickens with clinical
14
15 symptoms in china. *Viruses.* **2015**, *7*, 887–898.
- 16
17 (11) Webster, R. G.; Bean, W. J.; Gorman, O. T.; Chambers, T. M.; Kawaoka, Y.
18
19 Evolution and ecology of influenza A viruses. *Microbiol. Rev.* **1992**, *56*, 152–179.
- 20
21 (12) Choi, W. S.; Baek, Y. H.; Kwon, J. J.; Jeong, J. H.; Park, S. J.; Kim, Y. I.; Yoon, S.
22
23 W.; Hwang, J.; Kim, M. H.; Kim, C. J.; Webby, R. J.; Choi, Y. K.; Song, M. S. Rapid
24
25 acquisition of polymorphic virulence markers during adaptation of highly pathogenic
26
27 avian influenza H5N8 virus in the mouse. *Sci. Rep.* **2017**, *7*, 40667.
- 28
29 (13) Li, Y. T.; Ko, H. Y.; Lee, C. C.; Lai, C. Y.; Kao, CL.; Yang, C.; Wang, W. B.;
30
31 King, C. C. Phenotypic and genetic characterization of avian influenza H5N2 viruses
32
33 with intra-and inter-duck variations in Taiwan. *PLoS One.* **2015**, *10*, e0133910.
- 34
35 (14) Bi, Y.; Liu, J.; Xiong, H.; Zhang, Y.; Liu, D.; Liu, Y.; Gao, G. F.; Wang, B. A new
36
37 reassortment of influenza A (H7N9) virus causing human infection in Beijing, 2014.
38
39 *Sci Rep.* **2016**, *27*, 26624.
- 40
41 (15) Zhou, J.; Wu, J.; Zeng, X.; Huang, G.; Zou, L.; Song, Y.; Gopinath, D.; Zhang, X.;
42
43 Kang, M.; Lin, J.; Cowling, B. J.; Lindsley, W. G.; Ke, C.; Peiris, J. S.; Yen, H. L.
44
45 Isolation of H5N6, H7N9 and H9N2 avian influenza A viruses from air sampled at
46
47 live poultry markets in China, 2014 and 2015. *Euro. Surveill.* **2016**, *21* (35), 30331.
- 48
49 (16) Khurana, S.; Sasono, P.; Fox, A.; Nguyen, V. K.; Le, Q. M.; Pham, Q. T.; Nguyen,
50
51 T. H.; Nguyen, T. L.; Horby, P.; Golding, H. H5N1-SeroDetect EIA and rapid test: a
52
53
54
55
56
57
58
59
60

1
2
3 novel differential diagnostic assay for serodiagnosis of H5N1 infections
4 and surveillance. *J. Virol.* **2011**, *85*, 12455–12463.

5
6
7 (17) Couceiro, J. N. S. S.; Paulson, J. C.; Baum, L. G. Influenza virus strains
8 selectively recognize sialyloligosaccharides on human respiratory epithelium, the role
9 of the host cell in selection of hemagglutinin receptor specificity. *Virus Res.* **1993**, *29*,
10 155–165.

11
12
13 (18) Wu, Y.; Wu, Y.; Tefsen, B.; Shi, Y.; Gao, G. F. Bat-derived influenza-like viruses
14 H17N10 and H18N11. *Trends Microbiol.* **2014**, *22*, 183–191.

15
16 (19) (a) An, J.; Lee, D. C.; Law, A. H.; Yang, C. L.; Poon, L. L.; Lau, A. S.; Jones, S. J.
17 A novel small-molecule inhibitor of the avian influenza H5N1 virus determined
18 through computational screening against the neuraminidase. *J. Med. Chem.* **2009**, *52*,
19 2667–2672. (b) Bouvier, N. M.; Palese, P. The biology of influenza viruses. *Vaccine*
20 **2008**, *26*, D49–D53.

21
22 (20) Yang, J.; Liu, S.; Du, L.; Jiang, S. A new role of neuraminidase (NA) in the
23 influenza virus life cycle: implication for developing NA inhibitors with novel
24 mechanism of action. *Rev. Med. Virol.* **2016**, *26*, 242–250.

25
26 (21) Loregian, A.; Mercorelli, B.; Nannetti, G.; Compagnin, C.; Palù, G. Antiviral
27 strategies against influenza virus: towards new therapeutic approaches. *Cell. Mol. Life*
28 *Sci.* **2014**, *71*, 3659–3683.

29
30 (22) McClellan, K.; Perry, C. M. Oseltamivir: a review of its use in influenza. *Drugs*
31 **2001**, *61*, 263–283.

32
33 (23) (a) von Itzstein, M.; Wu, W. Y.; Kok, G. B.; Pegg, M. S.; Dyason, J. C.; Jin, B.;
34 Van Phan, T.; Smythe, M. L.; White, H. F.; Oliver, S. W. Rational design of potent
35 sialidase-based inhibitors of influenza virus replication. *Nature* **1993**, *363*, 418–423. (b)
36
37
38
39
40
41
42
43
44
45
46
47
48
49
50
51
52
53
54
55
56
57
58
59
60
Dunn, C. J.; Goa, K. L. Zanamivir: a review of its use in influenza. *Drugs* **1999**, *58*,

1
2
3 761–784.

4
5 (24) Kubo, S.; Tomozawa, T.; Kakuta, M.; Tokumitsu, A.; Yamashita, M. Laninamivir
6
7 prodrug CS-8958, a long-acting neuraminidase inhibitor, shows superior
8
9 anti-influenza virus activity after a single administration. *Antimicrob. Agents*
10
11 *Chemother.* **2010**, *54*, 1256–1264.

12
13 (25) Anuwongcharoen, N.; Shoombuatong, W.; Tantimongcolwat, T.; Prachayasittikul,
14
15 V.; Nantasenamat, C. Exploring the chemical space of influenza neuraminidase
16
17 inhibitors. *PeerJ.* **2016**, *19*, e1958.

18
19 (26) Memoli, M. J.; Hrabal, R. J.; Hassantoufighi, A.; Eichelberger, M. C.;
20
21 Taubenberger, J. K. Rapid selection of oseltamivir-and peramivir-resistant pandemic
22
23 H1N1 virus during therapy in 2 immunocompromised hosts. *Clin. Infect. Dis.* **2010**,
24
25 *50*, 1252–1255.

26
27 (27) Collins, P. J.; Haire, L. F.; Lin, Y. P.; Liu, J. F.; Russell, R. J.; Walker, P. A.;
28
29 Skehel, J. J.; Martin, S. R.; Hay, A. J.; Gamblin, S. J. Crystal structures of
30
31 oseltamivir-resistant influenza virus neuraminidase mutants. *Nature* **2008**, *453*,
32
33 1258–1262.

34
35 (28) Dapat, C.; Kondo, H.; Dapat, I. C.; Baranovich, T.; Suzuki, Y.; Shobugawa, Y.;
36
37 Saito, K.; Saito, R.; Suzuki, H. Neuraminidase inhibitor susceptibility profile of
38
39 pandemic and seasonal influenza viruses during the 2009-2010 and 2010-2011
40
41 influenza seasons in Japan. *Antiviral Res.* **2013**, *99*, 261–269.

42
43 (29) Samson, M.; Pizzorno, A.; Abed, Y.; Boivin, G. Influenza virus resistance to
44
45 neuraminidase inhibitors. *Antiviral Res.* **2013**, *98*, 174–185.

46
47 (30) Russell, R. J.; Haire, L. F.; Stevens, D. J.; Collins, P. J.; Lin, Y. P.; Blackburn, G.
48
49 M.; Hay, A. J.; Gamblin, S. J.; Skehel, J. J. The structure of H5N1 avian influenza
50
51 neuraminidase suggests new opportunities for drug design. *Nature* **2006**, *443*, 45–49.
52
53
54
55

- 1
2
3 (31) Han, N.; Mu, Y. Plasticity of 150-loop in influenza neuraminidase explored by
4 hamiltonian replica exchange molecular dynamics simulations. *PLoS. One.* **2013**, *8*,
5 e60995.
6
7
8
9 (32) Wu, Y.; Qin, G.; Gao, F.; Liu, Y.; Vavricka, C. J.; Qi, J.; Jiang, H.; Yu, K.; Gao, G.
10 F. Induced opening of influenza virus neuraminidase N2 150-loop suggests an
11 important role in inhibitor binding. *Sci. Rep.* **2013**, *3*, 1551.
12
13 (33) Li, Q.; Qi, J.; Zhang, W.; Vavricka, C. J.; Shi, Y.; Wei, J.; Feng, E.; Shen, J.; Chen,
14 J.; Liu, D.; He, J.; Yan, J.; Liu, H.; Jiang, H.; Teng, M.; Li, X.; Gao, G. F. The 2009
15 pandemic H1N1 neuraminidase N1 lacks the 150-cavity in its active site. *Nat. Struct.*
16 *Mol. Biol.* **2010**, *17*, 1266–1268.
17
18 (34) Xie, Y.; Xu, D.; Huang, B.; Ma, X.; Qi, W.; Shi, F.; Liu, X.; Zhang, Y.; Xu, W.
19 Discovery of N-substituted oseltamivir derivatives as potent and selective inhibitors
20 of H5N1 influenza neuraminidase. *J. Med. Chem.* **2014**, *57*, 8445–8458.
21
22 (35) You, Q.; Huang, K.; Du, G.; Liu, A.; Li, C. Derivatives of oseltamivir, and method
23 and medical application thereof. C.N. Patent CN 102659615, **2012**.
24
25 (36) Mohan, S.; McAtamney, S.; Haselhorst, T.; von Itzstein, M.; Pinto, B. M.
26 Carbocycles related to oseltamivir as influenza virus group-1-specific neuraminidase
27 inhibitors. Binding to N1 enzymes in the context of virus-like particles. *J. Med. Chem.*
28 **2010**, *53*, 7377–7391.
29
30 (37) Rudrawar, S.; Dyason, J. C.; Rameix-Welti, M. A.; Rose, F. J.; Kerry, P. S.;
31 Russell, R. J.; van der Werf, S.; Thomson, R. J.; Naffakh, N.; von Itzstein, M. Novel
32 sialic acid derivatives lock open the 150-loop of an influenza A virus group-1 sialidase.
33 *Nat. Commun.* **2010**, *1*, 113–119. (38) Lin, C. H.; Chang, T. C.; Das, A.; Fang, M. Y.;
34 Hung, H. C.; Hsu, K. C.; Yang, J. M.; von Itzstein, M.; Mong, K. K.; Hsu, T. A.; Lin,
35 C. C. Synthesis of acylguanidine zanamivir derivatives as neuraminidase inhibitors
36
37
38
39
40
41
42
43
44
45
46
47
48
49
50
51
52
53
54
55
56
57
58
59
60

- 1
2
3 and the evaluation of their bio-activities. *Org. Biomol. Chem.* **2013**, *11*, 3943–3948.
- 4
5 (39) Adabala, P. J.; LeGresley, E. B.; Bance, N.; Niikura, M.; Pinto, B. M.
6
7 Exploitation of catalytic site and 150 cavity for design of influenza A neuraminidase
8
9 inhibitors. *J. Org. Chem.* **2013**, *78*, 10867–10877.
- 10
11 (40) Amaro, R. E.; Minh, D. D.; Cheng, L. S.; Lindstrom, W. M. Jr.; Olson, A. J.; Lin,
12
13 J. H.; Li, W. W.; Mc. Cammon, J. A. Remarkable loop flexibility in avian influenza
14
15 N1 and its implications for antiviral drug design. *J. Am. Chem. Soc.* **2007**, *129*,
16
17 7764–7765.
- 18
19 (41) Rudrawar, S.; Dyason, J. C.; Rameix-Welti, M. A.; Rose, F. J.; Kerry, P. S.;
20
21 Russell, R. J.; van der Werf, S.; Thomson, R. J.; Naffakh, N.; von Itzstein, M. Novel
22
23 sialic acid derivatives lock open the 150-loop of an influenza A virus group-1 sialidase.
24
25 *Nat. Commun.* **2010**, *1*, 113.(42) Amaro, R. E.; Swift, R. V.; Votapka, L.; Li, W. W.;
26
27 Walker, R. C.; Bush, R. M. Mechanism of 150-cavity formation in influenza
28
29 neuraminidase. *Nat. Commun.* **2011**, *2*, 388.
- 30
31 (43) Hsu, K. C.; Hung, H. C.; Huang, Fu, W. C.; Sung, T. Y.; Eight, Lin, T.; Fang, M.
32
33 Y.; Chen, I. J.; Pathak, N.; Hsu, J. T.; Yang, J. M. Identification of Neuraminidase
34
35 Inhibitors Against Dual H274Y/I222R Mutant Strains. *Sci. Rep.* **2017**, *7*, 12336.
- 36
37 (44) Vavricka, C. J.; Li, Q.; Wu, Y.; Qi, J.; Wang, M.; Liu, Y.; Gao, F.; Liu, J.; Feng, E.;
38
39 He, J.; Wang, J.; Liu, H.; Jiang, H.; Gao, G. F. Structural and functional analysis of
40
41 laninamivir and its octanoate prodrug reveals group specific mechanisms for influenza
42
43 NA inhibition. *Plos Pathog* **2011**, *7*, e1002249.
- 44
45 (45) Samson, M.; Pizzorno, A.; Abed, Y.; Boivin, G. Influenza virus resistance to
46
47 neuraminidase inhibitors. *Antivir. Res.* **2013**, *98*, 174–185.
- 48
49 (46) Abed Y.; Baz M.; Boivin G. Impact of neuraminidase mutations conferring
50
51 influenza resistance to neuraminidase inhibitors in the N1 and N2 genetic
52
53
54
55
56
57
58
59
60

1
2
3 backgrounds. *Antivir Ther.* **2006**, *11*, 971–976.

4
5 (47) Wetherall N. T.; Trivedi T.; Zeller J.; Hodges-Savola C.; McKimm-Breschkin J.
6
7 L.; Zambon M.; Hayden F. G. Evaluation of neuraminidase enzyme assays using
8
9 different substrates to measure susceptibility of influenza virus clinical isolates to
10
11 neuraminidase inhibitors: report of the neuraminidase inhibitor susceptibility network.
12
13 *J. Clin. Microbiol* **2003**, *41*, 742-750.

14
15 (48) Sriwilaijaroen, N.; Magesh, S.; Imamura, A.; Ando, H.; Ishida, H.; Sakai, M.;
16
17 Ishitsubo, E.; Hori, T.; Moriya, S.; Ishikawa, T.; Kuwata, K.; Odagiri, T.; Tashiro, M.;
18
19 Hiramatsu, H.; Tsukamoto, K.; Miyagi, T.; Tokiwa, H.; Kiso, M.; Suzuki, Y. A novel
20
21 potent and highly specific inhibitor against influenza viral N1-N9 neuraminidases:
22
23 insight into neuraminidase-inhibitor interactions. *J. Med. Chem.* **2016**, *59*, 4563–4577.

24
25 (49) Schwaid, A. G.; Cornella-Taracido, I. Causes and significance of increased
26
27 compound potency in cellular or physiological contexts. *J. Med. Chem.* **2018**, *61*,
28
29 1767-1773.

30
31 (50). Dimova, D.; Bajorath, J. Rationalizing promiscuity cliffs. *Chem. Med. Chem.*
32
33 **2017**, *12*, 1–6.

34
35 (51). Stumpfe, D.; Hu, Y.; Dimova, D.; Bajorath, J. Recent progress in understanding
36
37 activity cliffs and their utility in medicinal chemistry. *J. Med. Chem.* **2014**, *57*, 18–28.

38
39 (52) Liu, A. L.; Wang, H. D.; Lee, S. M.; Wang, Y. T.; Du, G. H. Structure-activity
40
41 relationship of flavonoids as influenza virus neuraminidase inhibitors and their in
42
43 vitro anti-viral activities. *Bioorg. Med. Chem.* **2008**, *16*, 7141–7147.

44
45 (53) Shie, J. J.; Fang, J. M.; Wang, S. Y.; Tsai, K. C.; Cheng, Y. S.; Yang, A. S.; Hsiao,
46
47 S. C.; Su, C. Y.; Wong, C. H. Synthesis of tamiflu and its phosphonate congeners
48
49 possessing potent anti-influenza activity. *J. Am. Chem. Soc.* **2007**, *129*, 11892–11893.
50
51
52
53
54
55
56
57
58
59
60

1
2
3 (54) Muratore, G.; Goracci, L.; Mercorelli, B.; Foeglein, Á.; Digard, P.; Cruciani, G.;
4 Palù, G.; Loregian, A. Small molecule inhibitors of influenza A and B viruses that act
5 by disrupting subunit interactions of the viral polymerase. *Proc. Natl. Acad. Sci. USA.*
6
7
8
9 **2012**, *109*, 6247–6252.

10
11 (55) Massari, S.; Nannetti, G.; Goracci, L.; Sancineto, L.; Muratore, G.; Sabatini, S.;
12 Manfroni, G.; Mercorelli, B.; Cecchetti, V.; Facchini, M.; Palù, G.; Cruciani, G.;
13 Loregian, A.; Tabarrini, O. Structural investigation of
14 cycloheptathiophene-3-carboxamide derivatives targeting influenza virus polymerase
15 assembly. *J. Med. Chem.* **2013**, *56*, 10118–10131.

16
17 (56) Massari, S.; Nannetti, G.; Desantis, J.; Muratore, G.; Sabatini, S.; Manfroni, G.;
18 Mercorelli, B.; Cecchetti, V.; Palù, G.; Cruciani, G.; Loregian, A.; Goracci, L.;
19 Tabarrini, O. A broad anti-influenza hybrid small molecule that potently disrupts the
20 interaction of polymerase acidic protein-basic protein 1 (PA-PB1) subunits. *J. Med.*
21 *Chem.* **2015**, *58*, 3830–3842.

22
23 (57) Lepri, S.; Nannetti, G.; Muratore, G.; Cruciani, G.; Ruzziconi, Mercorelli, B.;
24 Palù, G.; Cruciani, G.; Loregian, A.; Goracci, L. Optimization of small-molecule
25 inhibitors of influenza virus polymerase: from thiophene-3-carboxamide to polyamido
26 scaffolds. *J. Med. Chem.* **2014**, *57*, 4337–4350.

27
28 (58) Maestro Schrödinger, LLC, New York, NY, **2014**.

29
30 (59) LigPrep Schrödinger, LLC, New York, NY, **2014**.

31
32 (60) Yang, H.; Carney, P. J.; Mishin, V. P.; Guo, Z.; Chang, J. C.; Wentworth, D. E.;
33 Gubareva, L. V.; Stevens, J. Molecular characterizations of surface proteins
34 hemagglutinin and neuraminidase from recent H5Nx avian influenza viruses. *J Virol.*
35
36
37
38
39
40
41
42
43
44
45
46
47
48
49
50
51
52
53 **2016**, *90*, 5770–5784.

54
55 (61) Gubareva, L. V.; Sleeman, K.; Guo, Z.; Yang, H.; Hodges, E.; Davis, C. T.;

1
2
3 Baranovich, T.; Stevens, J. Drug susceptibility evaluation of an influenza A(H7N9)
4 virus by analyzing recombinant neuraminidase proteins. *The Journal of infectious*
5 *diseases* **2017**, *216*, (suppl_4), S566–S574.
6
7

8
9 (62) Sastry, G. M.; Adzhigirey, M.; Day, T.; Annabhimoju, R.; Sherman, W. Protein
10 and ligand preparation: parameters, protocols, and influence on virtual screening
11 enrichments. *J Comput Aid. Mol. Des.* **2013**, *27*, 221–234.
12
13

14
15 (63) Li, H.; Robertson, A. D.; Jensen, J. H. Very fast empirical prediction and
16 rationalization of protein pKa values. *Proteins* **2005**, *61*, 704–721.
17
18

19
20 (64) Friesner, R. A.; Banks, J. L.; Murphy, R. B.; Halgren, T. A.; Klicic, J. J.; Mainz,
21 D. T.; Repasky, M. P.; Knoll, E. H.; Shelley, M.; Perry, J. K.; Shaw, D. E.; Francis, P.;
22 Shenkin, P. S. Glide: A new approach for rapid, accurate docking and scoring. 1.
23 Method and assessment of docking accuracy. *J. Med. Chem.* **2004**, *47*, 1739–1749.
24
25
26

27
28 (65) Frisch, M. J.; Trucks, G. W.; Schlegel, H. B.; Scuseria, G. E.; Robb, M. A.;
29 Cheeseman, J. R.; Scalmani, G.; Barone, V.; Mennucci, B.; Petersson, G. A.; Nakatsuji,
30 H.; Caricato, M.; Li, X.; Hratchian, H. P.; Izmaylov, A. F.; Bloino, J.; Zheng, G.;
31 Sonnenberg, J. L.; Hada, M.; Ehara, M.; Toyota, K.; Fukuda, R.; Hasegawa, J.; Ishida,
32 M.; Nakajima, T.; Honda, Y.; Kitao, O.; Nakai, H.; Vreven, T.; Montgomery, J. A.;
33 Peralta, J. E.; Ogliaro, F.; Bearpark, M.; Heyd, J. J.; Brothers, E.; Kudin, K. N.;
34 Staroverov, V. N.; Kobayashi, R.; Normand, J.; Raghavachari, K.; Rendell, A.; Burant,
35 J. C.; Iyengar, S. S.; Tomasi, J.; Cossi, M.; Rega, N.; Millam, J. M.; Klene, M.; Knox,
36 J. E.; Cross, J. B.; Bakken, V.; Adamo, C.; Jaramillo, J.; Gomperts, R.; Stratmann, R.
37 E.; Yazyev, O.; Austin, A. J.; Cammi, R.; Pomelli, C.; Ochterski, J. W.; Martin, R. L.;
38 Morokuma, K.; Zakrzewski, V. G.; Voth, G. A.; Salvador, P.; Dannenberg, J. J.;
39 Dapprich, S.; Daniels, A. D.; Farkas; Foresman, J. B.; Ortiz, J. V.; Cioslowski, J.; Fox,
40 D. J. Gaussian 09, Revision B.01. Wallingford CT, **2009**.
41
42
43
44
45
46
47
48
49
50
51
52
53
54
55

1
2
3 (66) Breneman, C. M.; Wiberg, K. B. Determining atom-centered monopoles from
4 molecular electrostatic potentials. The need for high sampling density in formamide
5 conformational analysis. *J. Comput. Chem.* **1990**, *11*, 361–373.
6
7

8
9 (67) Case, D. A.; Babin, V.; Berryman, J. T.; Betz, R. M.; Cai, Q.; Cerutti, D. S.;
10 Cheatham, T. E.; Darden, T. A.; Duke, R. E.; Gohlke, H.; Goetz, A. W.; Gusarov, S.;
11 Homeyer, N.; Janowski, P.; Kaus, J.; Kolossváry, I.; Kovalenko, A.; Lee, T. S.;
12 LeGrand, S.; Luchko, T.; Luo, R.; Madej, B.; Merz, K. M.; Paesani, F.; Roe, D. R.;
13 Roitberg, A.; Sagui, C.; Salomon-Ferrer, R.; Seabra, G.; Simmerling, C. L.; Smith, W.;
14 Swails, J.; Walker, J.; Wang, J.; Wolf, R. M.; Wu, X.; Kollman, P. A., {Amber 14}. 2014.
15
16

17 (68) Berendsen, H. J. C.; Postma, J. P. M.; van Gunsteren, W. F.; DiNola, A.; Haak, J.
18 R. Molecular dynamics with coupling to an external bath. *J. Chem. Phys.* **1984**, *81*,
19 3684–3690.
20
21

22 (69) Kang, D.; Fang, Z.; Huang, B.; Lu, X.; Zhang, H.; Xu, H.; Huo, Z.; Zhou, Z.; Yu,
23 Z.; Meng, Q.; Wu, G.; Ding, X.; Tian, Y.; Daelemans, D.; De Clercq, E.; Pannecouque,
24 C.; Zhan, P.; Liu, X. Structure-based optimization of thiophene[3,2-d]pyrimidine
25 derivatives as potent HIV-1 non-nucleoside reverse transcriptase inhibitors with
26 improved potency against resistance-associated variants. *J. Med. Chem.* **2017**, *60*,
27 4424–4443.
28
29
30
31
32
33
34
35
36
37
38
39
40
41
42
43
44
45
46
47
48
49
50
51
52
53
54
55
56
57
58
59
60

Table of Contents Graphic

